Dietary fat disrupts a commensal-host lipid network that promotes metabolic health

Highlights

- A Turicibacter species isolated from spore-forming bacteria promotes metabolic health
- Turicibacter and protective spore-forming bacteria suppress host ceramide metabolism
- Colonization of Turicibacter is reduced by a high-fat diet
- Lipids produced by *Turicibacter* prevent obesity and metabolic dysfunction

Authors

Kendra Klag, Darci Ott, Trevor S. Tippetts, ..., Scott A. Summers, W. Zac Stephens, June L. Round

Correspondence

june.round@path.utah.edu

In brief

Klag et al. identified that *Turicibacter*, a spore-forming bacteria, promotes leanness by producing unique lipids that suppress host ceramides and reduce fat uptake. High-fat diets lower *Turicibacter* levels and its protective effects, but supplementation with *Turicibacter* or *Turicibacter* lipids prevents obesity, revealing a therapeutic lipid metabolic circuit between bacteria and host.





Article

Dietary fat disrupts a commensal-host lipid network that promotes metabolic health

Kendra Klag,¹ Darci Ott,¹ Trevor S. Tippetts,² Rebekah J. Nicolson,² Sean M. Tatum,² Kaylyn M. Bauer,¹ Emmanuel Stephen-Victor,¹ Allison M. Weis,¹ Rickesha Bell,¹ James Weagley,³ J. Alan Maschek,²,⁴ Dai Long Vu,⁵ Stacey Heaver,⁵ Ruth Ley,⁵ Ryan O'Connell,¹ William L. Holland,² Scott A. Summers,² W. Zac Stephens,¹ and June L. Round¹,6,*

¹Department of Pathology, Division of Microbiology & Immunology, Huntsman Cancer Institute, University of Utah School of Medicine, Salt Lake City, UT 84112, USA

SUMMARY

The microbiota influences metabolic health; however, few specific microbial molecules and mechanisms have been identified. We isolated a *Turicibacter* strain from a community of spore-forming bacteria that promotes leanness in mice. Human metagenomic analysis demonstrates reduced *Turicibacter* abundance in individuals with obesity. Similarly, a high-fat diet reduces *Turicibacter* colonization, preventing its weight-suppressive effects, which can be overcome with continuous *Turicibacter* supplementation. Ceramides accumulate during a high-fat diet and promote weight gain. Transcriptomics and lipidomics reveal that the spore-forming community and *Turicibacter* suppress host ceramides. *Turicibacter* produces unique lipids, which are reduced during a high-fat diet. These lipids can be transferred to host epithelial cells, reduce ceramide production, and decrease fat uptake. Treatment of animals with purified *Turicibacter* lipids prevents obesity, demonstrating that bacterial lipids can promote host metabolic health. These data identify a lipid metabolic circuit between bacteria and host that is disrupted by diet and can be targeted therapeutically.

INTRODUCTION

Metabolic diseases, including type 2 diabetes (T2D), cardiovascular disease, and fatty liver disease, affect billions worldwide. ^{1,2} Obesity and a Western diet high in fat and sugar place individuals at significant risk for these diseases. ^{3–6} Diet influences many factors that contribute to obesity, including the composition of the microbiota. ⁷ The microbiota's role in obesity and metabolic diseases has been demonstrated by transferring microbiotas from obese donors into lean germ-free (GF) mice, causing weight gain. ^{8–10} A key feature of the microbiota in individuals with obesity is decreased microbial species diversity, which also occurs in animals on a high-fat diet (HFD). ^{11,12} However, GF mice lacking all gut bacteria are protected from weight gain associated with an HFD. ¹³ Collectively, these data suggest that some microbes promote weight gain while others restrict it.

Toll-like receptors (TLRs) recognize microbial ligands and signal through the adaptor protein MyD88. Our group showed that mice lacking MyD88 in T cells (T-MyD88^{-/-}) became spontaneously obese on a normal diet, with weight gain accelerated on an HFD.¹⁴ This weight gain in the T-MyD88^{-/-} mice was

dependent on the microbiota. Specifically, T-MyD88^{-/-} mice had a reduction in spore-forming (SF) bacteria, largely composed of *Clostridia* and *Erysipelotrichaceae* species. Supplementing T-MyD88^{-/-} mice with the SF community, isolated from wild-type (WT) mice, decreased small intestine (SI) fat absorption and weight gain. The SF community was complex, with over 80 different species in the community, and the specific organisms driving metabolic protection remain unknown.

Excess dietary fats are stored as triglycerides in adipose tissue, but an adipocyte has a finite lipid storage capacity. When lipids accumulate in tissue not suited for lipid storage, such as the liver, muscle, and blood vessels, it creates a toxic state that drives many metabolic diseases. Accumulation of ceramides, a type of sphingolipid, mediates many effects leading to metabolic disease. Elevated serum ceramide levels are found in individuals with obesity, T2D, and cardiovascular disease. Rablation of host ceramide-producing enzymes, including serine palmitoyltransferase 1 (SPTLC1) and dihydroceramide desaturase 1 (DES1), protects mice from developing fatty liver and insulin resistance, while overexpression of acid ceramidase (ASAH1), which degrades ceramides, leads to improved

²Department of Nutrition and Integrative Physiology, College of Health, University of Utah, Salt Lake City, UT 84112, USA

³Department of Medicine, Division of Infectious Diseases, Edison Family Center for Genome Sciences & Systems Biology, Washington University School of Medicine, St. Louis, MO 63110, USA

⁴Metabolomics Core Research Facility, University of Utah, Salt Lake City, UT 84112, USA

⁵Department of Microbiome Science, Max Planck Institute for Biology, Tübingen, Germany

⁶Lead contact

^{*}Correspondence: june.round@path.utah.edu https://doi.org/10.1016/j.cmet.2025.10.007



Cell Metabolism Article

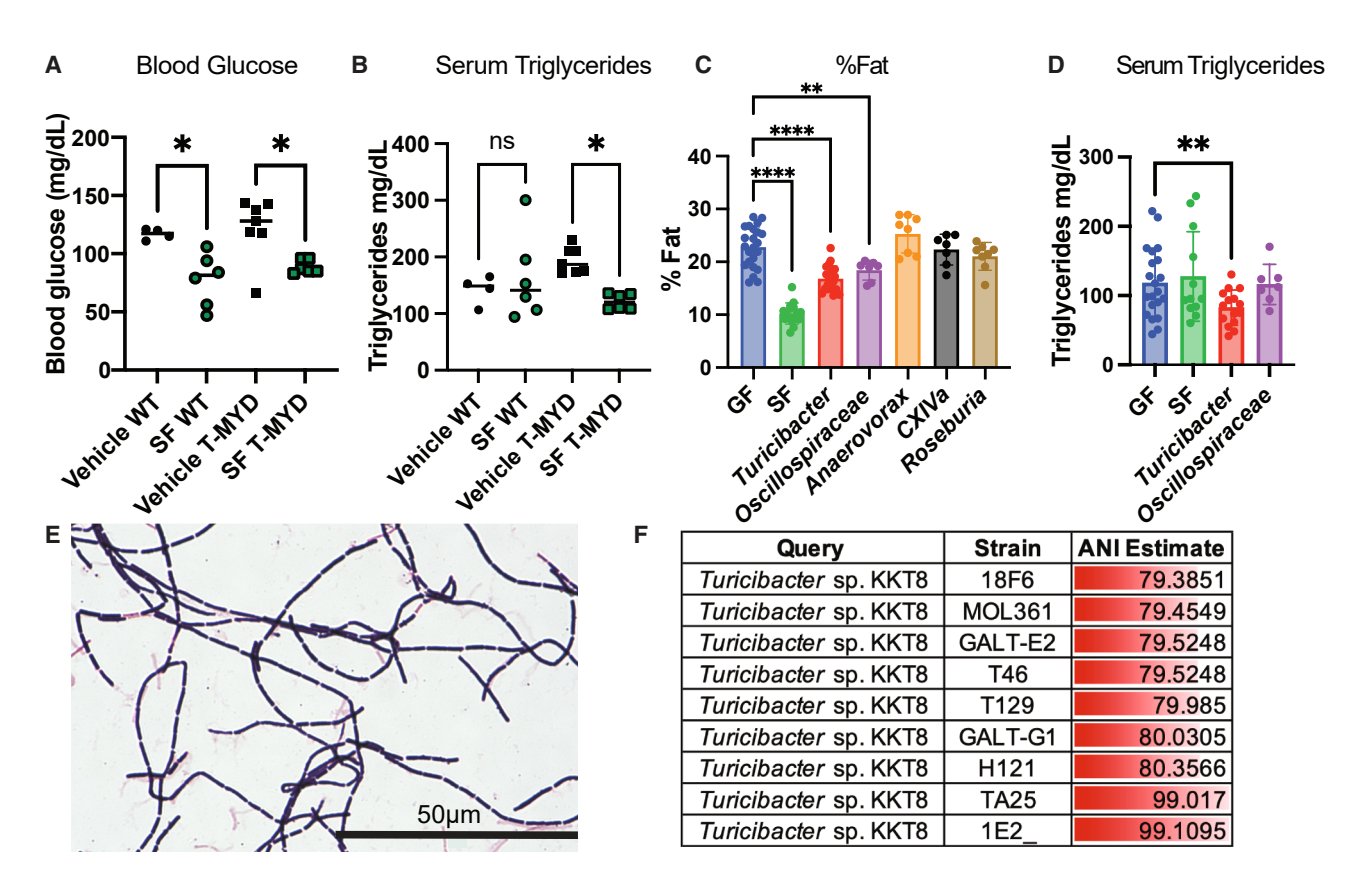


Figure 1. Identification of leanness-inducing microbes from the SF community

(A and B) (A) Fasting blood glucose and (B) serum triglycerides of 8-week-old male WT and T-MyD88 $^{-/-}$ mice on an HFD supplemented with SF for 2 months (WT, n = 10; T-Myd88 $^{-/-}$, n = 13).

- (C) Body fat % by NMR of GF mice colonized with SF (n = 16), Turicibacter (n = 20), Oscillospiraceae (n = 7), Anaerovorax (n = 8), CXIVa (n = 7), Roseburia (n = 8), or GF (n = 23). Representative of 5 independent experiments.
- (D) Fasting serum triglycerides of SF (n = 12), Turicibacter (n = 15), Oscillospiraceae (n = 7), or GF (n = 23) mice. Representative of 3 independent experiments.
- (E) Gram stain of Turicibacter at $100\times$; scale bar, $50~\mu m.$
- (F) ANI $\mathit{Turicibacter}$ KKT8 comparisons to other $\mathit{Turicibacter}$ strains.

*p < 0.05, **p < 0.01, ***p < 0.001, ****p < 0.0001; (A–C) one-way ANOVA with multiple comparisons was used to calculate statistical significance. Data are presented as mean \pm SD.

systemic metabolism.^{24–26} Ceramides alter host metabolism to promote intestinal lipid uptake and storage while decreasing glucose uptake and oxidation.^{16,17} Identification of mechanisms to control host ceramide accumulation could help treat many metabolic diseases.

The microbiota is known to influence host metabolism, but specific bacterial-driven mechanisms remain unclear. Sphingolipid production is conserved in Bacteroidetes, including *Bacteroides* and some *Proteobacteria*. ^{27,28} Knocking out SPT in *Bacteroides thetaiotaomicron* abolished bacterial sphingolipid production and altered sphingolipids produced by the host. ²⁹ Reduced bacterial sphingolipids are associated with inflammatory bowel disease (IBD), suggesting commensal sphingolipids influence host lipid metabolism. ³⁰ Additionally, *Bacteroides*-derived sphingolipids can transfer to host cells and modify cell metabolism. ³¹ While these few studies demonstrate that the microbiota can modify host lipid and sphingolipid metabolism, it is unclear if this is physiologically relevant or if organisms from the Bacillota/Firmicutes phyla can produce bioactive lipids that impact host biology.

RESULTS

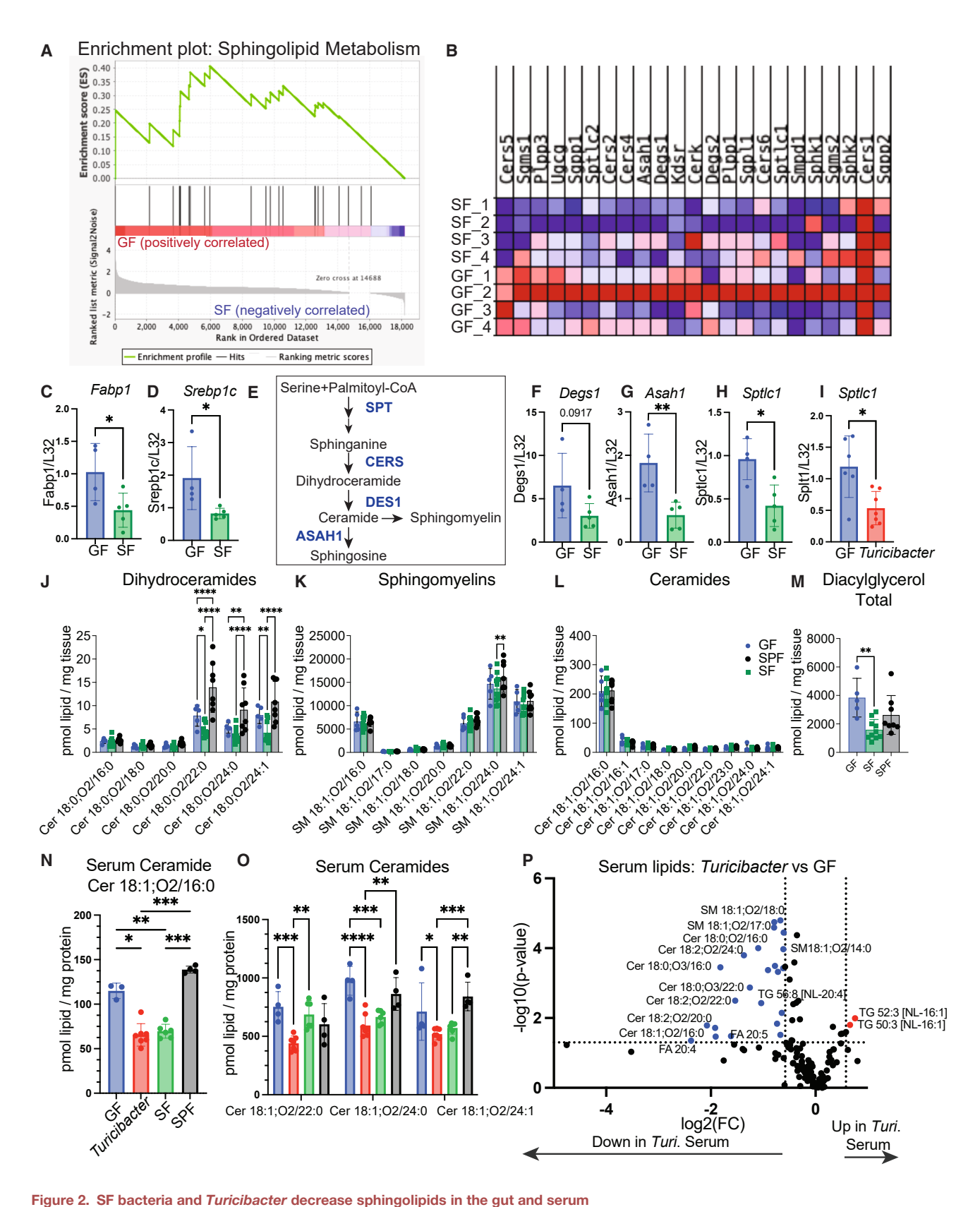
A single member of the SF community, *Turicibacter*, improves metabolic health

Our previous studies demonstrated that T-MyD88^{-/-} animals developed microbiota-dependent metabolic disease. These animals lacked many SF bacteria, and supplementing with the complex SF community reduced weight gain on an HFD.¹⁴ However, other aspects of metabolic health were not analyzed. After placing WT or T-MyD88^{-/-} mice on an HFD, animals were gavaged with the SF community for 8 weeks. SF-fed animals had significantly reduced fasting blood glucose in both WT and T-MyD88^{-/-} animals compared with PBS-treated animals (Figure 1A). Serum triglycerides were reduced in SF-treated T-MyD88^{-/-} animals, but not WT animals, suggesting SF supplementation was most effective in animals lacking SF bacteria (Figure 1B). Thus, treatment with the SF community can improve multiple parameters of metabolic health.

The metabolically protective SF community contains at least 80 bacterial species (NCBI taxonomy) present at >0.1% relative

Article





(A and B) RNA-seq of LCM of duodenal villi and crypts from GF and SF animals (GF, n = 4; SF, n = 4). Gene set enrichment analysis (GSEA) wiki pathways of sphingolipid metabolism integrated pathways.



Cell Metabolism Article

abundance. To identify protective members, individual bacteria from the SF community were isolated, cultured, and used to monocolonize GF mice. Mice colonized with the SF community had lower body fat compared with GF animals (Figure 1C). Of the five distinct isolates, *Turicibacter* sp. and *Oscillosporaceae* sp. conferred a lean phenotype similar to SF mice and significantly reduced the body fat compared with GF mice (Figure 1C). Neither isolate alone reduced body fat as much as the full SF community (Figure 1C). Interestingly, the *Turicibacter* sp. isolate lowered fasting serum triglycerides, whereas neither the whole SF community nor the *Oscillosporaceae* sp. isolate did (Figure 1D), demonstrating that different commensals confer distinct metabolic effects. Interestingly, *Turicibacter* comprises 12.9% abundance of the SF community (Figure S1A).

Turicibacter is a genus of anaerobic Gram-positive SF bacteria that form elongated rods and filaments (Figure 1E). Few Turicibacter strains have been isolated and sequenced. To compare our isolate, Turicibacter KKT8, to known strains, its genome was sequenced and assembled. Average nucleotide identity (ANI) comparisons revealed that Turicibacter KKT8 is most closely related to the other mouse-derived isolates, Turicibacter 1E2 and TA25 (~99% ANI), but only 80% ANI to the T. sanguinis species (Figure 1F).32,33 Recent studies have begun to shed light on Turicibacter's function. One study identified that T. sanguinis MOL361 reduced serum triglycerides, while the other observed no differences in metabolic parameters. 32,34 Turicibacter sequences have also been identified in ancient non-industrialized human microbiomes, suggesting a long association with humans.³⁴ Collectively, our data identify *Turicibacter* KKT8 as an SF community member capable of reducing fat accumulation and serum triglycerides. 32,34

The SF community and *Turicibacter* downregulate sphingolipid metabolism within the SI and serum

The SI is the major site of nutrient acquisition. Composed of specialized enterocytes with connections to the pancreas and the liver, it plays a direct role in metabolic regulation. ^{35,36} The SI microbiota helps regulate host lipid metabolism. ³⁷ While some organisms can upregulate fatty acid uptake, we previously showed that the SF community downregulates fatty acid uptake, though the mechanism was unclear. ¹⁴ To understand how the SF community impacts intestinal epithelial cell (IEC) biology, laser capture microdissection (LCM) was used to isolate villi and crypt cells from the SI duodenum (SID) of GF and SF community-colonized mice. Gene expression was extensively altered upon colonization with the SF community (Figure S2A). We previously found that the SF community modulates intestinal CD36, a gene regulated by ceramides. ^{14,24} A focused metabolic pathway

analysis revealed that many genes involved in sphingolipid, including ceramide metabolism, were downregulated in SF vs. GF and specific pathogen-free (SPF) mice (Figures 2A, 2B, and S2B), though not all sphingolipid genes were affected (Figures S2C and S2D).

Sphingolipids are a large class of lipids with many unique species that have diverse physiologic properties throughout the body.³⁸ Ceramides, a class of sphingolipids, are elevated in obesity, serve as a marker for the risk of cardiovascular disease, exacerbate metabolic disease, and are regulated by the microbiota. 16,39,40 Since RNA sequencing (RNA-seq) indicated altered ceramide metabolism, we used qPCR to confirm SF-induced changes in the SID of SF and GF animals. Consistent with the RNA-seq analysis, Fabp1 and Srebp-1c were downregulated in SF mice (Figures 2C and 2D). Both Fabp1 and Srebp-1c are known to be regulated by ceramides and are important in lipid metabolism.^{24,41} FABP1 binds long-chain fatty acids and regulates lipid metabolism and transport, while SREBP-1c is a key transcription factor involved in de novo lipogenesis. Other genes, including Degs1, Asah1, and Sptlc1, involved in sphingolipid biosynthesis and degradation as depicted in Figure 2E, were also downregulated in SF-colonized animals (Figures 2F-2H). Notably, Turicibacter KKT8 colonization similarly decreased Sptlc1 expression in the SID (Figure 2I). Ceramides have been shown to regulate dietary lipid uptake in the gut, supporting a role for SF and Turicibacter KKT8 in suppressing ceramide metabolism.41

Targeted lipidomics of the SID was performed to determine if SF colonization influences host lipid metabolism. Interestingly, SF animals have decreased dihydroceramides compared with GF mice (Figure 2J). While minimal changes in sphingomyelins and no changes in ceramides were observed (Figures 2K and 2L), this may reflect the importance of ceramide function within the gut. 41,42 Looking more broadly at lipids, we see that SF colonization compared with GF conditions modulates many other lipid species, including decreasing total diacylglycerides (Figures 2M, S2E, and S2F). The changes in SF compared with GF suggest that it is not just the loss of microbes but the presence of certain microbes that can modulate the abundances of host sphingolipids. Based on this, our results demonstrate that SF bacteria can modulate sphingolipid and lipid metabolism within the gut.

Serum ceramides are a predictor of cardiovascular disease, which is a significant comorbidity and cause of mortality in individuals with obesity. ^{39,43} Strikingly, colonization with *Turicibacter* KKT8 or the SF community lowers serum ceramides (Figures 2N and 2O). *Turicibacter* KKT8 monocolonization lowered multiple serum lipids, including dihydroceramides,

⁽C-E) qPCR on SID of GF or SF mice for (C) Fabp 1, (D) Srebp 1c, and (E) sphingolipid synthesis pathway (GF, n = 4; SF, n = 5; Turicibacter, n = 7). Black represents lipids, and blue represents enzymes.

⁽F-I) qPCR on SID of GF or SF or Turicibacter-colonized mice for (F) Des1, (G) Asha1, and (H and I) Sptlc1.

⁽J–M) Quantification of lipids in the SID of GF, SF, and SPF mice (GF, n = 5; SF, n = 8; SPF, n = 8). (J) Dihydroceramides. (K) Sphingomyelins. (L) Ceramides. (M) Diacylglycerides.

⁽N and O) Ceramides in the serum of GF, SF, Turicibacter-colonized, and SPF mice (GF, n = 4; Turicibacter, n = 7; SF, n = 6; SPF, n = 4).

⁽P) Volcano plot of differentially abundant lipids between *Turicibacter* and GF serum. Red dots showing lipid species significantly increased in serum of *Turicibacter* mice, and blue dots showing lipid species significantly decreased in serum of *Turicibacter* mice, with dotted lines showing >1.5-fold change and p < 0.05. GF, n = 4; *Turicibacter*, n = 7.

^{*}p < 0.05, **p < 0.01, ****p < 0.001, *****p < 0.0001; (C, D, and F-I) unpaired t test; (J-O) ordinary one-way ANOVA with multiple comparisons was used to calculate statistical significance. Data are presented as mean \pm SD.

Article



ceramides, sphingomyelins, phytoceramides, hexosylceramides, and phosphatidylcholine (Figures 2P and S2G–S2K). The vast downregulation of serum lipids suggests that *Turicibacter* KKT8 can influence both gut and systemic lipid metabolism. These data support previous observations of *Turicibacter sp.* and expand on the impact of *Turicibacter* sp. on the host serum lipidome. Collectively, these data have identified that one bacterium, *Turicibacter* KKT8 from the complex SF community, can confer leanness, reduce serum triglycerides, and suppress sphingolipid metabolism, revealing it as a crucial player in metabolic health.

An HFD impairs the colonization and growth of Turicibacter

Diet plays a central role in metabolic diseases and significantly influences gut microbiota composition. ^{7,45} Our findings that *Turicibacter* KKT8 promotes leanness and metabolic health in mice led us to investigate *Turicibacter* levels in humans with obesity. Using the GMrepo curated human metagenomic database, we found that *Turicibacter* levels were markedly lower in individuals with obesity (Figure 3A), consistent with several other studies. ^{46–48} Taken together, these data suggest that reduced abundance of *Turicibacter* colonization is associated with individuals with obesity.

Placing animals on an HFD is an established way to model obesity and metabolic disease. ⁴⁹ While monocolonization with *Turicibacter* KKT8 or the SF community on a normal chow (NC) diet results in leaner mice compared with GF controls (Figure 1C), this effect is lost during HFD (Figure 3B). Microbiotas of humans with obesity and animals on HFD are both associated with decreased microbial diversity, suggesting diet may directly affect *Turicibacter* abundance. ^{47,50–52} To test this, *Turicibacter* KKT8 monocolonized animals were placed on NC or HFD, and *Turicibacter* KKT8 abundance was analyzed along the intestinal tract. Strikingly, HFD almost eliminated *Turicibacter* KKT8 from the SI (Figures 3C–3E) and significantly reduced it in the lower gastrointestinal (GI) tract (Figures 3F and 3G), despite it being the only organism within the gut. These data demonstrate that a diet high in fat can directly reduce *Turicibacter* colonization.

Palmitate (PA) is the building block for sphingolipid metabolism and the major saturated fat component of an HFD.⁵³ To determine if PA influences the growth of Turicibacter KKT8, Turicibacter KKT8 was grown in increasing concentrations of PA (Figure 3H). Growth was significantly reduced in PA-containing media compared with control (Figure 3H) and halted when PA was added to active cultures (Figure 3I). PA is not necessarily toxic to Turicibacter KKT8, as the bacteria resumes growth when removed from PA-containing media (Figure 3J). In fact, RNA-seq of Turicibacter KKT8 cultures revealed many PAinduced transcriptional changes. The most highly upregulated genes included transcription factors involved in stress response (MerR family) and metabolic shifts (TetR/AcrR family), as well as many spore proteins (Figure 3K; Table S1). This suggests PA is inducing a different metabolic state that is potentially stressful and inducing spore formation. Failure to grow in the presence of PA is not a general feature of all types of bacteria, as only Turicibacter KKT8 and Bacteroides uniformis, but not Desulfovibrio desulfuricans and Escherichia coli Nissle (E. coli Nissle), were sensitive to the addition of PA to the growth media (Figure 3L). These data demonstrate that humans with obesity have reduced colonization of *Turicibacter* and that dietary fat can prevent its persistence in the gut, underscoring the critical role of diet in shaping the microbiota.

Continuous supplementation of *Turicibacter* KKT8 prevents obesity and reduces host ceramides during an HFD

The loss of *Turicibacter* colonization in humans with obesity and in animals on an HFD diet suggested that obesity could develop, in part, due to the absence of Turicibacter. To elevate Turicibacter under the unfavorable environment of an HFD, we tested repeated supplementation of Turicibacter KKT8. Previously, we discovered that T-MyD88^{-/-} mice had a reduction in SF bacteria, including Turicibacter, which correlated with increased weight. 14 Weight gain in T-MyD88-/- mice was accelerated by feeding a 45% HFD over 8 weeks. Because of this precedence using 45% HFD and because the 45% HFD may offer a more realistic reflection of calories consumed by humans in the setting of obesity, we used 45% HFD for all studies in this paper.⁵ T-MyD88^{-/-} mice were placed on HFD and given oral *Turici*bacter KKT8 5 days a week. Supplemented animals gained less weight and had reduced body fat, smaller inguinal white adipose tissue (iWAT), fasting glucose, and serum ceramides (Figures 4A–4F and S3A–S3D). Thus, in the T-MyD88^{-/-} genetic model that develops microbiota-dependent obesity, oral supplementation with Turicibacter KKT8 could slow weight gain and metabolic changes associated with an HFD. Similarly, WT SPF mice also benefited metabolically from Turicibacter KKT8 on HFD, showing reduced weight gain, iWAT mass, and multiple serum lipids, including triglycerides and ceramides (Figures 4G-4L and S3E-S3H). Turicibacter KKT8 supplementation in WT animals on an HFD also lowered many lipids in the duodenum, including ceramides, sphingosine, and sphingomyelin, as well as numerous fatty acids and phosphatidylcholines (Figures S3J-S3N). We have seen that Turicibacter KKT8 must be continuously supplemented to provide metabolic protection, as the HFD abolishes the abundance of Turicibacter in the feces, but daily supplementation increases its abundance to similar levels as what is in our SPF community at baseline (Figure S3I). These results highlight that Turicibacter KKT8 supplementation can suppress adverse metabolic effects of HFD consumption, thus identifying a potential therapeutic intervention for individuals with obesity and metabolic diseases.

Turicibacter lipid metabolism is modulated by the presence of dietary lipids

An HFD negatively impacts the growth and metabolically protective capacity of *Turicibacter*, and its colonization or supplementation impacts host lipid and sphingolipid metabolism, suggesting lipid metabolism plays a key role in *Turicibacter* KKT8 biology. We considered that a high lipid environment could be toxic to *Turicibacter*; however, *Turicibacter* KKT8 cultures rebounded after removal from PA-rich media (Figure 3J). To test if dietary lipids modify *Turicibacter* metabolism, we grew *Turicibacter* KKT8, *B. uniformis*, *D. desulfuricans*, and *E. coli Nissle* in media containing PA with a terminal alkyne group (PAA). Bacteria were grown in PAA-rich media overnight and washed and treated with click chemistry to attach a fluorophore to the



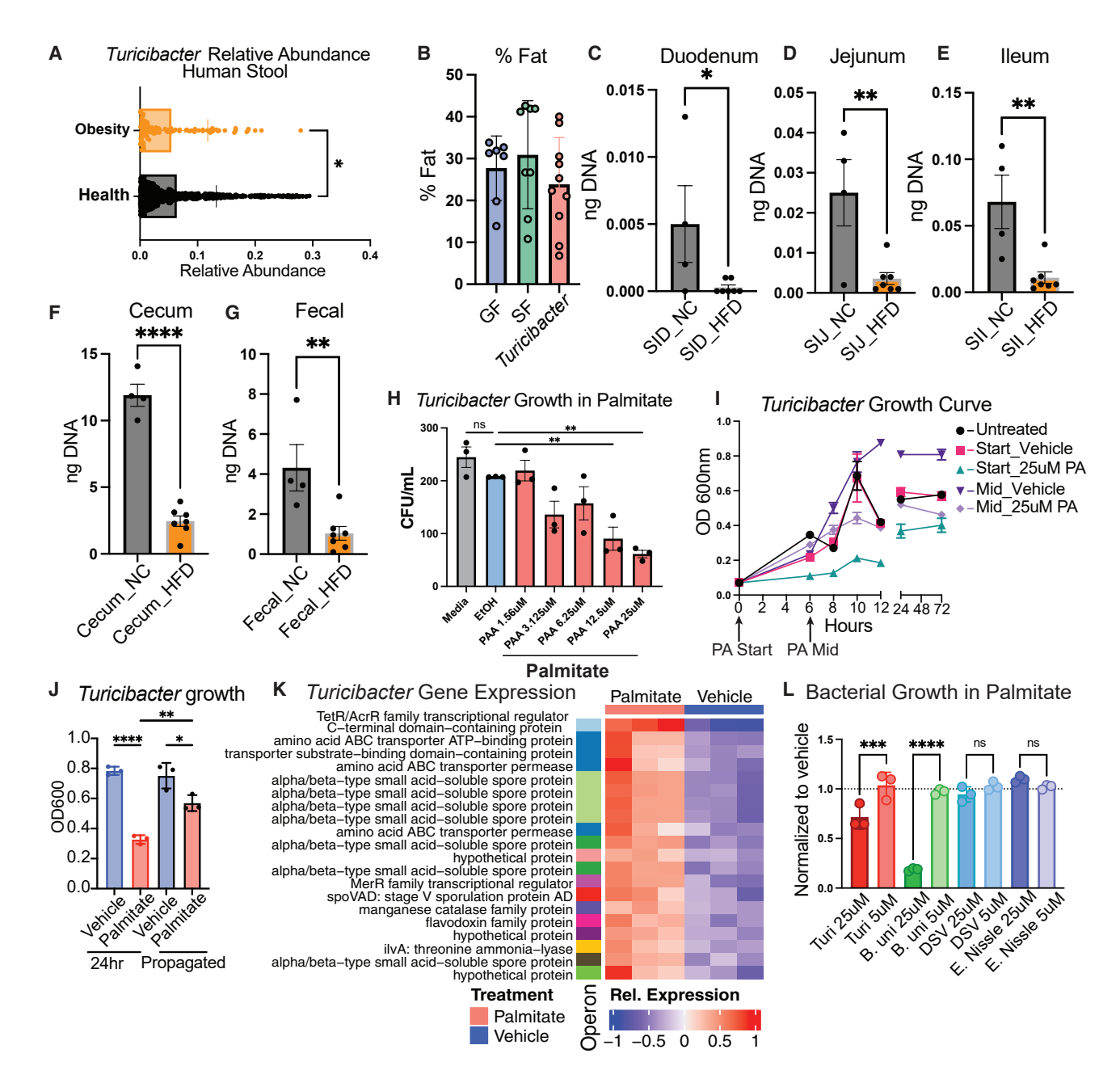


Figure 3. Lipids are detrimental to Turicibacter growth

(A) Relative abundance of the *Turicibacter* genus in human fecal metagenomic sequencing in humans with obesity (*n* = 115) or healthy (*n* = 1,000) from GMrepo. (B) Body fat % by NMR of GF (*n* = 7), SF (*n* = 8), or *Turicibacter* (*n* = 10 on HFD).

- (C–G) Quantity of 16s bacterial DNA in *Turicibacter* monocolonized mice on NC or HFD along the intestinal tract (NC, n = 4; HFD, n = 7). (C) Duodenum. (D) Jejunum. (E) Ileum. (F) Cecum. (G) Feces.
- (H) Colony-forming unit (CFU)/mL growth of Turicibacter KKT8 in culture with PA and ethanol vehicle (n = 3 per condition).
- (I) Growth curve by OD 600 nm of Turicibacter KKT8 cultures (n = 3 per condition).
- (J) Growth of *Turicibacter* KKT8 during PA exposure and after it has been propagated into PA-free media (n = 3 per condition).
- (K) Heatmap of top 20 (by fold change) upregulated genes in *Turicibacter* KKT8 with PA treatment. Gene labels are the product annotation of each locus tag preceded by gene symbols, when available, in the gene's annotation. Genes with shared colors in the operon annotation on the left belong to the same predicted operon. Each column is a sample (n = 3, vehicle; n = 3, PA treated), and cell colors reflect regularized log-transformed expression values mean-centered in each row to show relative expression.
- (L) Growth of *Turicibacter* KKT8, *B. uniformis*, *D. desulfuricans*, and *E. coli Nissle* in 25 μ M PA normalized to ethanol vehicle (n=3 per condition). *p < 0.05, **p < 0.01, ***p < 0.001, ****p < 0.001. (A) Kolmogorov-Smirnov unpaired t test, (C–G) unpaired t tests, and (B, H, J, and L) ordinary one-way ANOVA with multiple comparisons were used to calculate statistical significance. Data are presented as mean \pm SD.

Article



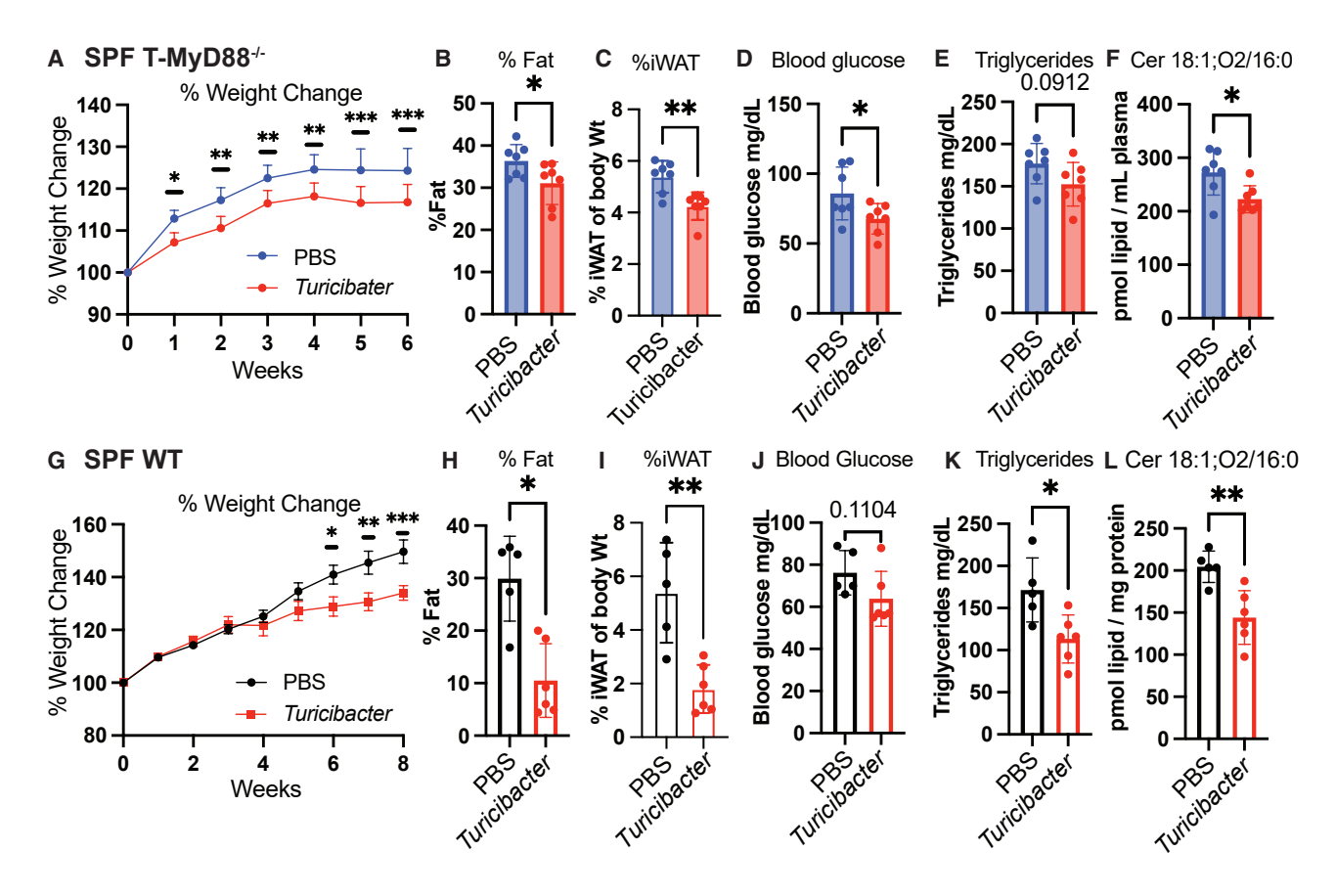


Figure 4. Continuous supplementation of Turicibacter is metabolically protective on an HFD

(A–F) 11-week-old male SPF T-Myd88 $^{-/-}$ mice gavaged with Turicibacter KKT8 for 6 weeks on an HFD (PBS, n = 7; Turicibacter, n = 7).

- (A) Change in body weight from baseline.
- (B) Body fat %.
- (C) iWAT weight relative to body weight.
- (D) Fasting blood glucose.
- (E) Fasting serum triglycerides.
- (F) Quantification of serum ceramides.
- (G-L) 6-week-old male SPF WT mice gavaged with Turicibacter KKT8 for 8 weeks on HFD (PBS, n = 5; Turicibacter, n = 6).
- (G) Change in body weight from baseline.
- (H) Body fat % by NMR.
- (I) iWAT weight relative to body weight.
- (J) Fasting blood glucose.
- (K) Fasting serum triglycerides.
- (L) Quantification of serum ceramides.

*p < 0.05, **p < 0.01, ****p < 0.001, ****p < 0.0001; (A and G) two-way ANOVA with multiple comparisons and (B–F and H–L) unpaired t test were used to calculate statistical significance. Data are presented as mean \pm SD.

PAA and analyzed by flow cytometry. Despite lipids being an important source of energy, only *Turicibacter* KKT8 and *B. uniformis*, but not *D. desulfuricans* and *E. coli Nissle*, were capable of taking up dietary PA (Figure 5A). *B. uniformis* and other Bacteroides species are known to take up PA.^{29,31} However, *Turicibacter* is not closely related to *Bacteroides*, and their capability of metabolizing dietary PA represents a novel feature for an organism among the *Bacillota* phyla of bacteria.

The reduced growth and function of *Turicibacter* KKT8 in PA suggest that host diet modifies *Turicibacter* lipid metabolism. Bacteria-derived lipids are increasingly recognized as bioactive metabolites, yet most bacterial lipidomes remain undefined. ⁵⁵ Classification of bacterial lipids remains challenging because

reference databases are built off eukaryote-derived lipids and only a few bacteria. *Turicibacter* KKT8's lipidome was characterized *in vitro* with or without PA using untargeted liquid chromatography-tandem mass spectrometry (LC-MS/MS). Consistent with a poorly characterized bacterial lipidome, only 5% of all lipids produced by *Turicibacter* KKT8 were annotated as calculated from the percent of annotated lipids from all MS hits (Tables S2 and S3); however, those that were annotated represent approximately two-thirds of the total lipid abundances produced by the bacteria. *Turicibacter* KKT8 produces a diverse lipid profile, distinct from *Bacteroides*. ⁵⁶ The *Turicibacter* KKT8 lipidome is dominated by monogalactosyldiacylglycerol (MGDG) and digalactosyldiacylglycerol (DGDG) lipids (Figures 5B, 5C, and S4A–S4D;



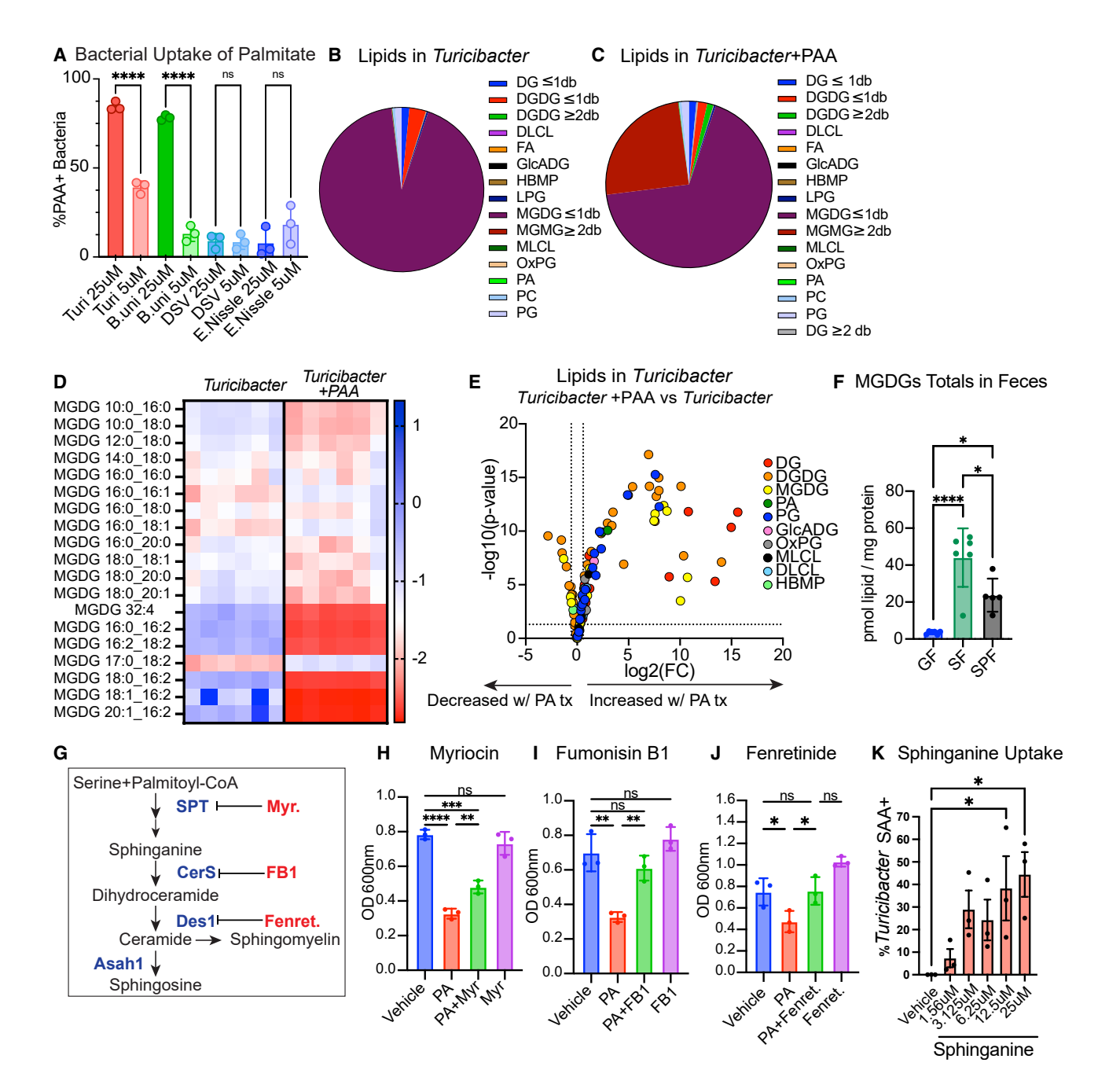


Figure 5. Turicibacter lipid metabolism is modulated by the presence of dietary lipids

- (A) Percent of bacteria PAA-positive (n = 3 per condition).
- (B and C) Pie chart of lipid abundances in (B) Turicibacter KKT8 and (C) Turicibacter + PAA. n = 3 per condition.
- (D) Heatmap of MGDG lipids in *Turicibacter* and *Turicibacter* + PAA. n = 3 per condition.
- (E) Volcano plot of lipids increased in *Turicibacter* treated with PAA (right) and decreased in *Turicibacter* treated with PAA (left). Colors represent different lipid classes, and dotted lines represent fold change >1.5 and p < 0.05. *Turicibacter*, n = 6; *Turicibacter* + PAA, n = 6.
- (F) Abundance of total MGDG lipids in feces from GF, SF, or SPF mice (GF, n = 6; SF, n = 6; SPF, n = 5).
- (G) Sphingolipid synthesis pathway schematic. Red represents pharmacological inhibitors act.
- (H–J) Growth of Turicibacter ± PA and (H) 5 μM myriocin, (I) 5 μM fumonisin B1, and (J) 5 μM fenretinide. n = 3 per condition.
- (K) Turicibacter uptake of Alkyne sphinganine (SAA). n = 3 per condition.
- p' < 0.05, p' < 0.01, p' < 0.01, p' < 0.001, p' < 0.001; (A, F, and H-K) ordinary one-way ANOVA with multiple comparisons was used to calculate statistical significance. Data are presented as mean p' = 0.001; (A, F, and H-K) ordinary one-way ANOVA with multiple comparisons was used to calculate statistical significance.

Cer 18:2;O2/24:0-Cer 18:2;O2/24:1-Cer 19:1;O2/24:1-





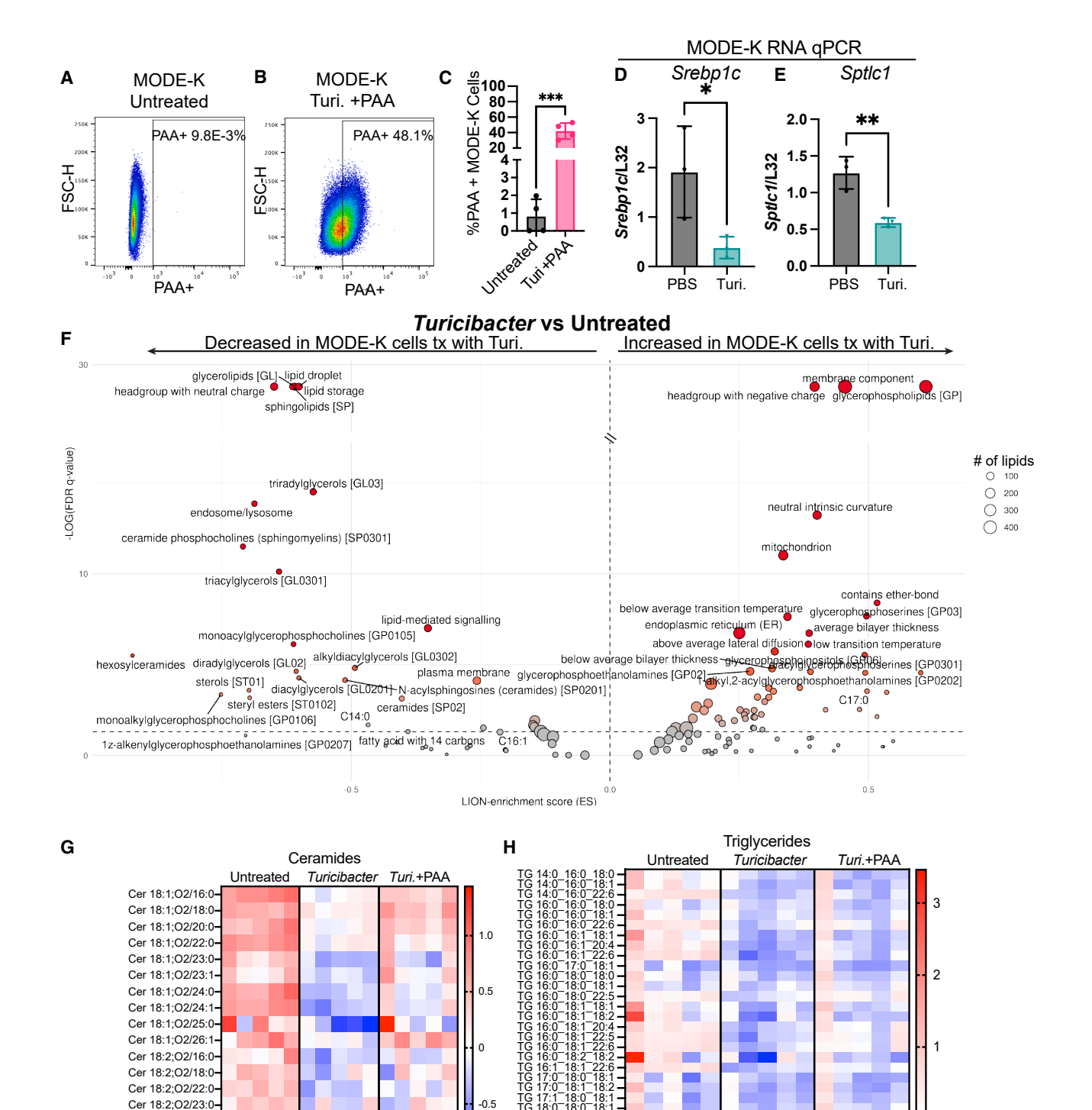


Figure 6. *Turicibacter* lipids transfer into epithelial cells and downregulate ceramide and lipid metabolism *in vitro* (A and B) Gating of PAA-negative and -positive MODE-K cells.

(C) PAA-positive MODE-K cells untreated or co-incubated with *Turicibacter* KKT8 grown in PAA (untreated, n = 4; Turi+PAA, n = 4).

(D) PAA-positive MODE-K cells untreated or co-incubated with Turicibacter KK18 grown in PAA (untreated, n = 4; Turi+PAA, n = 4). (D and E) qPCR on MODE-K cells treated with Turicibacter KK18 (D) Srebp1 and (E) Sptlc1.



Cell Metabolism Article

Tables S2 and S3) and numerous other fatty acids, including vaccenic acid, palmitoleic acid, and 11-eicosenoic acid (Figure S4E). Growth in PA-rich media significantly altered the Turicibacter lipidome, supporting that dietary lipids can alter the intrinsic metabolism of Turicibacter KKT8 (Figures 5B-5E). The addition of PA to the Turicibacter KKT8 culture upregulates many classes of lipids (Figure 5E). Notably, Turicibacter KKT8 grown in PA had increases in polyunsaturated MGDGs, DGDGs, diacylglycerols (DGs), and phosphatidylglycerols (PGs) (Figures S4B, S4D, and S5A-S5C). A handful of DGDG lipids, one species of MGDG lipids (MGDG 17:0_18:2), and several fatty acids decreased with PA treatment (Figures 5D, S4A-S4E, and S5A). It has been challenging to ascertain if PAA is directly used as a substrate, as the databases used for analysis presently are not coded to detect the presence of the PAA 16:3 lipid. The 16:3 could potentially make up lipids that are reported as a summary composition, like MGDG 32:4, but other-sized lipids are likely to contribute to its abundance. Because the quantities of MGDG and DGDG lipids in Turicibacter increase with the addition of PAA (Figures S4B and S4D), it is possible that the PAA added is being used as a substrate.

Consistent with *Turicibacter* KKT8's ability to produce numerous fatty acids, the *Turicibacter* KKT8 genome possesses many genes predicted to be involved in fatty acid synthesis (Figure S6). The lipids MGDGs and DGDGs contain polyunsaturated fatty acids (PUFAs) and monounsaturated fatty acids (MUFAs), which have many effects on host metabolism. ^{57–59} Certain MGDGs and DGDGs have been shown to have immunomodulatory and anti-cancer properties. ^{60,61} MGDG and DGDG lipids play a crucial role in membranes in plants and cyanobacteria. ^{62,63} Feces from SF-colonized mice, abundant with *Turicibacter*, showed a significant amount of MGDG lipids compared with GF and SPF mice (Figure 5F). These data demonstrate that *Turicibacter* KKT8 produces an abundance of lipids that are shaped by host dietary fat.

While Bacteroides are known to possess an SPT gene and produce sphingolipids, Bacillota have not been shown to share this capacity.^{27,28} Though MS did not detect known sphingolipids, 95% of the Turicibacter lipidome remains unannotated (Tables S2 and S3). Therefore, it is possible that Turicibacter produces sphingolipid-like molecules. To investigate this, hidden Markov models were used to identify proteins from Turicibacter KKT8 with homology to bacterial CerS and SPT proteins. Candidate proteins encoded in the Turicibacter KKT8 genome encoded domains with accuracy scores of 0.72 and 0.87 to the hidden Markov model (HMM) models of CerS (PTHR41368.orig.30.pir) and SPT proteins, respectively (Table S4). These corresponded with 68.6% similarity to the HMM-model consensus sequence over the 70 amino acid aligned region for CerS and 58% similarity over the 220 amino acid aligned region for SPT. This is in line with the sequence homology of other bacterial genes described in Turicibacter.44

To investigate if *Turicibacter* KKT8 possesses sphingolipid synthesis-like proteins, we tested whether bacterial growth responded to drugs known to selectively inhibit SPT (myriocin), ceramide synthase (fumonisin B1), and DES1 (fenretinide) (Figure 5G). While the presence of PA significantly reduced Turicibacter KKT8 growth, adding any of the three inhibitors rescued the PA-induced growth defect (Figures 5H-5J). Both myriocin and fumonisin B1 are naturally derived products produced by fungi that are highly specific for their targets and have structures similar to sphingolipids. Interestingly, mice fed fumonisin B1 have an increased abundance of Turicibacter in their microbiota.⁶⁴ Because these sphingolipid inhibitors, with established high specificity for sphingolipid-synthesizing lipids, have an effect on the growth of Turicibacter KKT8, it suggests that the enzymes and lipids produced by Turicibacter KKT8 have enough structural homology with sphingolipids that these sphingolipid inhibitors are allowed to bind. Furthermore, Turicibacter KKT8 can also take up sphinganine (Figure 5K). The ability to utilize sphinganine is largely restricted to Bacteroides bacteria, which are known to synthesize sphingolipids. Turicibacter has previously been identified to take up sphinganine. 65 Collectively, these data demonstrate that Turicibacter makes a multitude of known lipids, including fatty acids, and many unknown lipids that have yet to be annotated. It is possible that some of these lipids might be structurally similar to sphingolipids. Future investigations will be aimed at a deeper analysis of these lipids.

Turicibacter lipids enter IECs and modulate host ceramide metabolism

Bacteroides lipids have been shown to transfer to host cells and influence metabolism. ^{29,31} Given that *Turicibacter* KKT8 produces numerous lipid species, we tested whether its lipids could similarly transfer to host cells. *Turicibacter* KKT8 cultured PAA and applied it to a mouse SI cell line (MODE-K cells). Click chemistry was used to fluorescently label all MODE-K cells harboring *Turicibacter* KKT8-derived lipids and quantified using flow cytometry (Figures 6A and 6B). Over 40% of the MODE-K cells possessed bacterially labeled lipids (Figure 6C). Suggesting host epithelial cell uptake of lipids produced by *Turicibacter* KKT8.

Consistent with *in vivo* findings, Turicibacter KKT8 exposure reduced expression of Srebp1c and Sptlc1 in MODE-K cells (Figures 6D and 6E). Lipidomic and lipid ontology (LION) analysis of the MODE-K cells treated with *Turicibacter* KKT8 revealed a significant downregulation in lipid storage, triglycerides, sphingolipids, and ceramides (Figures 6F–6H). 66,67 This is consistent with our findings that *Turicibacter* KKT8 monocolonization or supplementation decreases serum triglycerides and ceramides (Figures 1D, 2N, 2O, 4F, 4K, and 4L). Specifically, ceramide 18:1;02/16:0—the most abundant in the SI (Figure 2L) and modulated *in vivo* by Turicibacter (Figures 4F and 4L)—was reduced in treated epithelial cells, but this effect was lost when

⁽F) Lipidomics data analyzed by LION volcano plot of MODE-K cells treated with Turicibacter KKT8 vs. untreated (untreated, n = 5; Turicibacter, n = 5). (G and H) Heatmap of normalized lipids from MODE-K cells untreated, treated with Turicibacter KKT8, or treated with Turicibacter KKT8 grown in PAA. (G) Ceramides. (H) Triglyceride.

^{*}p < 0.05, **p < 0.01, ***p < 0.001; (C–E) unpaired t tests were used to calculate statistical significance. Data are presented as mean ± SD.





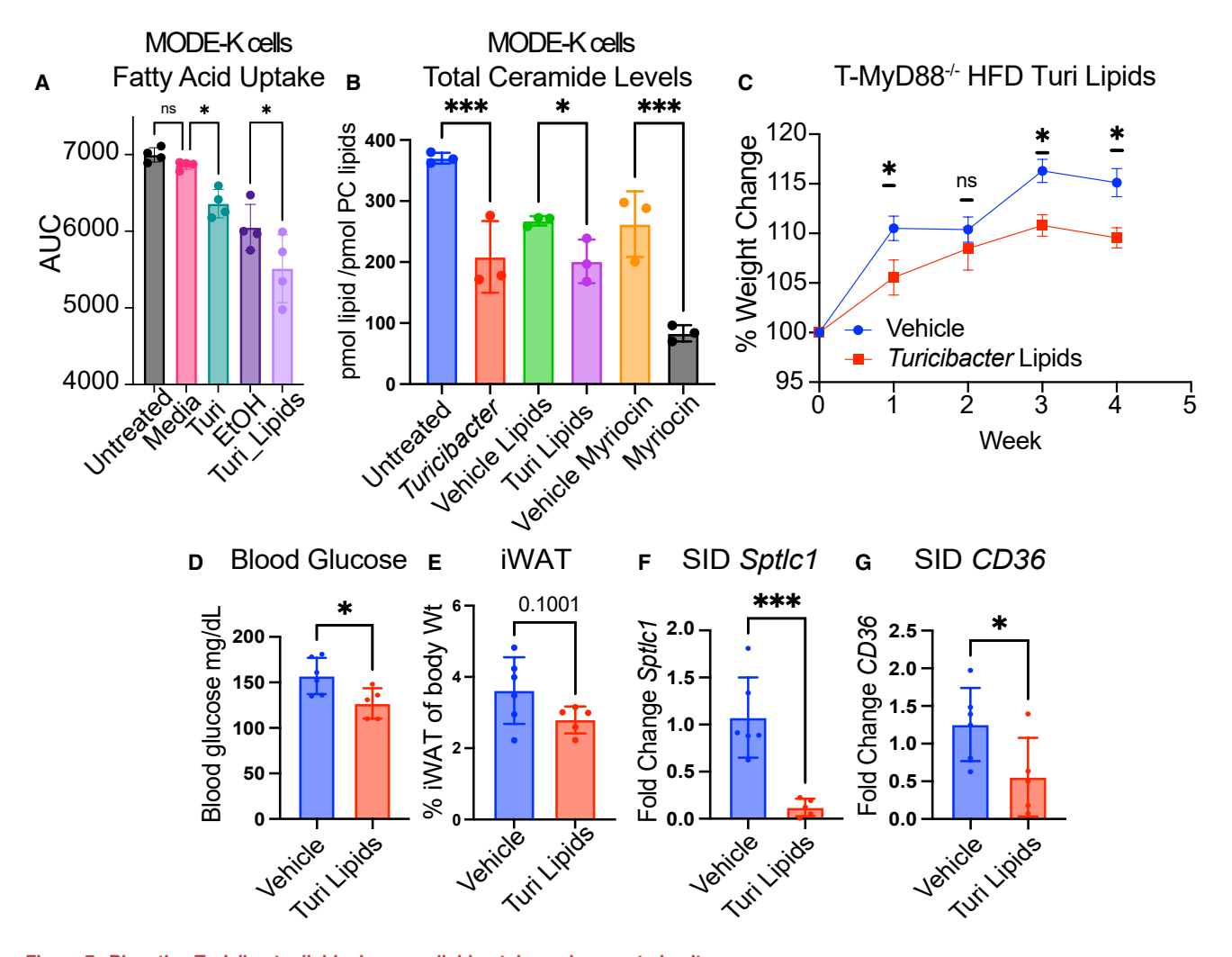


Figure 7. Bioactive Turicibacter lipids decrease lipid uptake and prevent obesity

(A) Area under the curve of fatty acid uptake assay in MODE-K cells untreated or treated with bacterial media, Turicibacter, ethanol vehicle, or Turicibacter lipids. n = 4 per condition.

- (B) Total ceramide levels from MODE-K cells treated with Turicibacter KKT8, Turicibacter-derived lipids, myriocin, and vehicles.
- (C–G) 11-week-old male SPF T-Myd88^{-/-} mice gavaged with *Turicibacter* lipids or vehicle for 4 weeks on an HFD (vehicle, n = 6; *Turicibacter*, n = 5).
- (C) Change in body weight from baseline.
- (D) Fasting blood glucose.
- (E) iWAT weight relative to body weight.
- (F and G) qPCR on SID of mice gavaged with PBS or Turicibacter lipids (F) Sptlc1 and (G) CD36.

*p < 0.05, **p < 0.01, ***p < 0.001, ****p < 0.0001; (A) ordinary one-way ANOVA with multiple comparisons, (B) two-way ANOVA with multiple comparisons, and (C–F) unpaired t tests were used to calculate statistical significance. Data are presented as mean \pm SD.

bacteria were grown in PAA (Figure 6G). These data demonstrate that *Turicibacter* KKT8 can deliver lipids to host epithelium, and this is associated with decreased host obesity-promoting ceramides. Moreover, the presence of dietary fat can modulate lipid metabolism within *Turicibacter* KKT8 that prevents downregulation of specific host ceramides.

Turicibacter lipids decrease fatty acid uptake in IECs and prevent obesity

Our data indicate that *Turicibacter* KKT8 can produce unique lipids that are transferred to epithelial cells and downregulate host ceramides linked to obesity. Previously, we showed the SF community reduces fatty acid uptake in the gut, and others

have shown ceramides promote uptake via CD36. 14,24 Collectively, these studies suggest *Turicibacter* KKT8 lipids may mediate its lean-promoting effects. To test this, fatty acid uptake was measured in MODE-K cells treated with *Turicibacter* KKT8 bacteria, *Turicibacter* KKT8 lipids, or their respective vehicle controls. As hypothesized, treatment of MODE-K cells with *Turicibacter* KKT8 or lipids from *Turicibacter* KKT8 significantly reduced fatty acid uptake (Figure 7A). Conditioned media (CM) from *Turicibacter* KKT8 also decrease fatty acid uptake in MODE-K cells (Figure S7). This suggests that the bioactive molecule in *Turicibacter* KKT8 is secreted. Additionally, total ceramide levels are decreased in MODE-K cells treated with *Turicibacter* KKT8-derived lipids, just like with whole *Turicibacter*



Cell MetabolismArticle

KKT8 treatment, and similar to cells treated with the SPT inhibitor myriocin (Figure 7B).

To assess *in vivo* effects of *Turicibacter* KKT8 lipids, T-MyD88^{-/-} mice were put on an HFD and gavaged with the *Turicibacter* KKT8 lipids. After 4 weeks, animals treated with *Turicibacter* KKT8 lipids gained significantly less weight, had lower fasting blood glucose, and had trendingly smaller inguinal fat pads (Figures 7C–7E). Additionally, treatment with *Turicibacter* KKT8 lipids significantly decreased SID *Sptlc1* and *CD36* expression (Figures 7F and 7G), consistent with ceramide pathway downregulation. Taken together, these data demonstrate that *Turicibacter* promotes metabolic health and prevents obesity through the production of bioactive lipids that act to downregulate host ceramide production.

DISCUSSION

Diet significantly impacts microbiota composition, yet little is known about how specific components affect individual organisms and their function. While a variety of metabolites are microbially derived, only a handful, such as short-chain fatty acids and secondary bile acids, have been well characterized. 55,68,69 Here we identify *Turicibacter* KKT8, a microbiota member diminished by HFD and in individuals with obesity, that produces a unique lipid capable of preventing obesity in the mammalian host, revealing a new class of molecules with metabolic benefits.

Individuals with obesity and animals on an HFD are associated with altered microbiotas, including reductions in specific taxa. 11,12,70 This suggests that metabolic disease might result from decreases in certain bacteria that promote health. We show Turicibacter colonization is reduced in humans with obesity. Prior studies have emphasized fiber as a microbial fuel, as much of the alterations in microbial composition observed during HFD feeding are thought to be due to a reduction in microbial-accessible carbohydrates like fiber. 71-74 We found that Turicibacter colonization is directly impacted by a major dietary lipid, PA. While Turicibacter utilizes PA, its growth is highly sensitive to PA but rebounds when PA is removed, suggesting an induction of a dormancy-like state. Supporting this, transcriptomics data of Turicibacter KKT8 show the upregulation of sporulation and stress response genes in response to PA. This induces a shift in Turicibacter metabolism that results in reductions in bacterial monounsaturated MGDG lipids and an increase in polyunsaturated MGDG lipids. MGDG and DGDG lipids are crucial in the membranes of photosynthetic bacteria, plants, and fungi. 63 Turicibacter does not photosynthesize but as an SF bacteria; thus, these lipids may play a role in spore formation, which has been reported in some fungi.⁷⁵ Increases in dietary fats may shift Turicibacter metabolism to alter its lifestyle to become a more dormant spore.

While it remains unclear why *Turicibacter* KKT8 responds to PA by altering its metabolism, our data demonstrate that this change in the *Turicibacter* KKT8 lipidome impacts host physiology. During normal conditions, *Turicibacter* KKT8 lipids are transferred to host epithelial cells and downregulate ceramides. Importantly, we demonstrated that exposure to *Turicibacter* KKT8-derived lipids tempers epithelial cell fatty acid uptake *in vitro* and prevents mice from gaining weight on an HFD while also lowering fasting blood glucose *in vivo*. While MGDGs are the

most abundant lipid species produced by *Turicibacter* KKT8, it remains unknown if these are the bioactive compounds acting on host cells. With only 5% of *Turicibacter* KKT8 lipids annotated, it leaves much of the *Turicibacter* lipidome unknown. The findings that PA-induced growth defects were reversed by sphingolipid pathway inhibitors and that *Turicibacter* takes up sphinganine suggest it may produce sphingolipid-like molecules that could interfere with host sphingolipid metabolism. Though *Turicibacter* is not yet genetically tractable, future work to characterize putative sphingolipid genes from *Turicibacter* using expression in other bacterial systems will be valuable. Overall, our results highlight *Turicibacter* lipids as a novel mode of host-microbe communication.

Studies of Turicibacter species have shown its growth and functions are sensitive to host serotonin. Similarly, our data suggest that dietary PA directly and independently changes Turicibacter lipid metabolites, as there is no serotonin in the in vitro culture.44 Other research has shown that monocolonization with varying Turicibacter sp. strains can modify circulating lipids by modulating bile acids. 32,44 Monocolonization with these strains did not impact inguinal fat mass; however, the effects of these strains in the setting of diet-induced obesity or in a more complex microbiota were not assessed. Turicibacter KKT8 is closely related to two other isolates that possess bile acid salt hydrolase (bsh) activity, and the KKT8 isolate also possesses two bsh genes. However, we find that prevention of obesity is dependent on the production of Turicibacter lipids, as purification and administration of the lipids from Turicibacter KKT8 was sufficient to reduce weight gain and thus acted independently of Turicibacter bsh activity. This identifies a new lipidmediated mechanism by which Turicibacter promotes metabolic health.

Defining a "healthy" or "diseased" microbiota remains a challenge, as individual variation is vast. Here, we see that the addition of the SF community or Turicibacter KKT8 to the T-MvD88^{-/-} mice lacking these microbes confers more benefit than in WT mice that already possess these microbes. Turicibacter abundance negatively correlates with dietary fats and adiposity, suggesting its potential as a biomarker. 52,76-78 However, increased Turicibacter levels have been linked to conditions like Parkinson's and depression, indicating strain-level effects. 79,80 Understanding how species- and strain-level variation in Turicibacter contributes to its impact on modulating health and disease will be vital in developing the therapeutic potential of Turicibacter. Through a personalized medicine approach, determining which individuals are deficient in Turicibacter and suffer from metabolic disease could reveal a patient population that would benefit most from Turicibacter-based therapeutics. Collectively, our data identify a novel bacterial-host lipid network that promotes host metabolic health and holds therapeutic promise.

Limitations of the study

While we have shown that *Turicibacter*-derived lipids can reduce obesity, other molecules and metabolites from *Turicibacter* may also contribute and warrant future investigation. Our data that demonstrates that *Turicibacter* lipids are directly transferred into host cells largely stems from *in vitro* studies and should be corroborated *in vivo* in future studies. This will require labeling

Article



and/or genetic manipulation studies in *Turicibacter*, which is not yet possible.

RESOURCE AVAILABILITY

Lead contact

Further information and requests for resources and reagents should be directed to and will be facilitated by the lead contact, June L. Round (june.round@path.utah.edu).

Materials availability

New reagents generated in this study are available by request to the lead contact.

Data and code availability

Host RNA-seq data from LCM are available under BioProject: PRJNA1122642 and GEO: GSE269607. *Turicibacter* culture RNA-seq data are available under BioProject: PRJNA1135257. SF community metagenomic sequences are available under BioProject: PRJNA1137940. No novel code was generated as part of this project. Scripts for processing and analysis of *Turicibacter* culture RNA-seq and metagenomics analysis of SF communities are available at https://github.com/RoundLab/Klag_TuricibacterLipids.

ACKNOWLEDGMENTS

The authors would like to thank members of the Round and O'Connell labs for their critical editing of this manuscript. We gratefully acknowledge the help from the University of Utah Flow Cytometry Facility, the Center for High Performance Computing, and the HCl bioinformatics core, and the authors thank Dan Cuthbertson of Agilent Technologies for assistance in implementing iterative exclusion in the tandem mass spectrometry experiments. This work was supported by NCl through award 5P30CA042014-24 and by NIH grants 5F30DK127846-04 to K.K.; F32CA243501 to A.M.W.; and R01DK124336, R01DK124317, and R01AT011423 to J.L.R. Grants from the Helmsley Foundation, Burrough's Welcome Foundation, and the Keck Foundation to J.L.R. also supported this work. Illustrations were made using BioRender.

AUTHOR CONTRIBUTIONS

K.K. was involved in all investigations, data analysis, and writing of this paper. D.O. was involved in the investigation for Figures 3H–3J, 3L, 4, 5A, 5H–5K, and 7B–7G and editing and writing. T.S.T., R.J.N., and S.N.T. helped with the investigation for lipidomic experiments. K.M.B., E.S.-V., A.M.W., and R. B. contributed to the investigation for animal experiments, microbiology work, writing, and conceptualization. J.W. performed formal analysis for Table S5. J.A.M. helped with investigation and formal analysis for lipidomic experiments. D.L.V., S.H., and R.L. contributed to conceptualization for bacterial lipidomic experiments. R.O. contributed resources. W.L.H. and S.A.S. contributed resources and conceptualization, investigation, and formal analysis of sequencing experiments. J.L.R. contributed conceptualization, funding acquisition, methodology, project administration, resources, supervision, analysis, and writing of this manuscript.

DECLARATION OF INTERESTS

The authors declare no competing interests.

STAR*METHODS

Detailed methods are provided in the online version of this paper and include the following:

- KEY RESOURCES TABLE
- EXPERIMENTAL MODEL AND SUBJECT DETAILS
 - Mice
- METHOD DETAILS
 - $\,\circ\,$ Colonization of mice with spore-forming microbes
 - o Culture Collection and Turicibacter Isolation

- Monocolonization experiments
- o Turicibacter Culturing
- o Bacterial growth and uptake of PA
- Diet treatment
- Metabolic phenotyping
- Blood Glucose measurement
- o Insulin ELISA
- Triglyceride assay
- o GMrepo
- o Turicibacter lipid extraction for gavaging
- In vitro experiments using mouse intestinal epithelial cells (MODE-K cells)
- o MODE-K cell co-incubation with Turicibacter
- Fatty Acid Uptake Assay
- o RNA isolation from small intestine for qPCR
- o Lipidomics
- o Lipidomics Chemicals
- o Lipidomics Sample Preparation
- O Lipidomics LC-MS Analysis
- o Lipidomics Data Processing and Quantification
- o Lipidomics Statistical Analysis and Visualization
- Lipidomics LION Analysis
- o Full List of Targeted Lipid MRM Transitions and Retention Times
- o Laser Capture Microdissection and RNA Seq
- o Host RNA seq analysis with GSEA
- o RNA seq and analysis of Turicibacter culture
- Turicibacter Genome Analysis for SPT, CerS and Fatty Acid Biosynthesis Pathway
- o Metagenomic sequencing and analysis of SF community
- QUANTIFICATION AND STATISTICAL ANALYSIS

SUPPLEMENTAL INFORMATION

Supplemental information can be found online at https://doi.org/10.1016/j.cmet.2025.10.007.

Received: July 26, 2024 Revised: May 21, 2025 Accepted: October 8, 2025

REFERENCES

- Swinburn, B.A., Kraak, V.I., Allender, S., Atkins, V.J., Baker, P.I., Bogard, J.R., Brinsden, H., Calvillo, A., De Schutter, O., Devarajan, R., et al. (2019). The global syndemic of obesity, undernutrition, and climate change: The Lancet Commission report. Lancet 393, 791–846. https:// doi.org/10.1016/S0140-6736(18)32822-8.
- Chew, N.W.S., Ng, C.H., Tan, D.J.H., Kong, G., Lin, C., Chin, Y.H., Lim, W.H., Huang, D.Q., Quek, J., Fu, C.E., et al. (2023). The global burden of metabolic disease: Data from 2000 to 2019. Cell Metab. 35, 414–428.e3. https://doi.org/10.1016/j.cmet.2023.02.003.
- Lusis, A.J., Attie, A.D., and Reue, K. (2008). Metabolic syndrome: from epidemiology to systems biology. Nat. Rev. Genet. 9, 819–830. https:// doi.org/10.1038/nrg2468.
- Mozaffarian, D., Benjamin, E.J., Go, A.S., Arnett, D.K., Blaha, M.J., Cushman, M., de Ferranti, S., Després, J.P., Fullerton, H.J., Howard, V. J., et al. (2015). Heart disease and stroke statistics–2015 update: a report from the American Heart Association. Circulation 131, e29–e322. https:// doi.org/10.1161/CIR.0000000000000152.
- Moreira, G.C., Cipullo, J.P., Ciorlia, L.A.S., Cesarino, C.B., and Vilela-Martin, J.F. (2014). Prevalence of metabolic syndrome: association with risk factors and cardiovascular complications in an urban population. PLoS One 9, e105056. https://doi.org/10.1371/journal.pone. 0105056



- 6. Polyzos, S.A., Kountouras, J., and Mantzoros, C.S. (2019). Obesity and nonalcoholic fatty liver disease: From pathophysiology to therapeutics. Metabolism 92, 82-97. https://doi.org/10.1016/j.metabol.2018.11.014.
- 7. Perler, B.K., Friedman, E.S., and Wu, G.D. (2023). The role of the gut microbiota in the relationship between diet and human health. Annu. Rev. Physiol. 85, 449-468. https://doi.org/10.1146/annurev-physiol-031522-092054.
- 8. Turnbaugh, P.J., Ley, R.E., Mahowald, M.A., Magrini, V., Mardis, E.R., and Gordon, J.I. (2006). An obesity-associated gut microbiome with increased capacity for energy harvest. Nature 444, 1027-1031. https:// doi.org/10.1038/nature05414.
- 9. Ridaura, V.K., Faith, J.J., Rey, F.E., Cheng, J., Duncan, A.E., Kau, A.L., Griffin, N.W., Lombard, V., Henrissat, B., Bain, J.R., et al. (2013). Gut microbiota from twins discordant for obesity modulate metabolism in mice. Science 341, 1241214. https://doi.org/10.1126/science.1241214.
- 10. Smith, M.I., Yatsunenko, T., Manary, M.J., Trehan, I., Mkakosya, R., Cheng, J., Kau, A.L., Rich, S.S., Concannon, P., Mychaleckyj, J.C., et al. (2013). Gut microbiomes of Malawian twin pairs discordant for kwashiorkor. Science 339, 548-554. https://doi.org/10.1126/science.
- 11. Davis, C.D. (2016). The gut microbiome and its role in obesity. Nutr. Today 51, 167-174. https://doi.org/10.1097/NT.000000000000167.
- 12. Lecomte, V., Kaakoush, N.O., Maloney, C.A., Raipuria, M., Huinao, K.D., Mitchell, H.M., and Morris, M.J. (2015). Changes in gut microbiota in rats fed a high fat diet correlate with obesity-associated metabolic parameters. PLoS One 10, e0126931. https://doi.org/10.1371/journal.pone.
- 13. Bäckhed, F., Manchester, J.K., Semenkovich, C.F., and Gordon, J.I. (2007). Mechanisms underlying the resistance to diet-induced obesity in germ-free mice. Proc. Natl. Acad. Sci. USA. 104, 979-984. https:// doi.org/10.1073/pnas.0605374104.
- 14. Petersen, C., Bell, R., Klag, K.A., Lee, S.H., Soto, R., Ghazaryan, A., Buhrke, K., Ekiz, H.A., Ost, K.S., Boudina, S., et al. (2019), T cellmediated regulation of the microbiota protects against obesity. Science 365, eaat9351. https://doi.org/10.1126/science.aat9351.
- 15. Yazıcı, D., and Sezer, H. (2017). Insulin resistance, obesity and lipotoxicity. Adv. Exp. Med. Biol. 960, 277-304. https://doi.org/10.1007/978-3-319-48382-5 12.
- 16. Chaurasia, B., and Summers, S.A. (2015). Ceramides lipotoxic inducers of metabolic disorders. Trends Endocrinol. Metab. 26, 538-550. https:// doi.org/10.1016/i.tem.2015.07.006.
- 17. Bikman, B.T., and Summers, S.A. (2011). Ceramides as modulators of cellular and whole-body metabolism. J. Clin. Invest. 121, 4222-4230. https://doi.org/10.1172/JCI57144.
- 18. Wigger, L., Cruciani-Guglielmacci, C., Nicolas, A., Denom, J., Fernandez, N., Fumeron, F., Marques-Vidal, P., Ktorza, A., Kramer, W., Schulte, A., et al. (2017). Plasma dihydroceramides are diabetes susceptibility biomarker candidates in mice and humans. Cell Rep. 18, 2269-2279. https://doi.org/10.1016/j.celrep.2017.02.019.
- 19. Anroedh, S., Hilvo, M., Akkerhuis, K.M., Kauhanen, D., Koistinen, K., Oemrawsingh, R., Serruys, P., van Geuns, R.J., Boersma, E., Laaksonen, R., and Kardys, I. (2018). Plasma concentrations of molecular lipid species predict long-term clinical outcome in coronary artery disease patients. J. Lipid Res. 59, 1729-1737. https://doi.org/10.1194/jlr. P081281.
- 20. Havulinna, A.S., Sysi-Aho, M., Hilvo, M., Kauhanen, D., Hurme, R., Ekroos, K., Salomaa, V., and Laaksonen, R. (2016). Circulating ceramides predict cardiovascular outcomes in the population-based FINRISK 2002 Cohort. Arterioscler. Thromb. Vasc. Biol. 36, 2424-2430. https:// doi.org/10.1161/ATVBAHA.116.307497.
- 21. Laaksonen, R., Ekroos, K., Sysi-Aho, M., Hilvo, M., Vihervaara, T., Kauhanen, D., Suoniemi, M., Hurme, R., März, W., Scharnagl, H., et al. (2016). Plasma ceramides predict cardiovascular death in patients with stable coronary artery disease and acute coronary syndromes beyond

- LDL-cholesterol. Eur. Heart J. 37, 1967-1976. https://doi.org/10.1093/ eurhearti/ehw148.
- 22. Meikle, P.J., Wong, G., Barlow, C.K., Weir, J.M., Greeve, M.A., MacIntosh, G.L., Almasy, L., Comuzzie, A.G., Mahaney, M.C., Kowalczyk, A., et al. (2013). Plasma lipid profiling shows similar associations with prediabetes and type 2 diabetes. PLoS One 8, e74341. https:// doi.org/10.1371/journal.pone.0074341.
- 23. Lemaitre, R.N., Yu, C., Hoofnagle, A., Hari, N., Jensen, P.N., Fretts, A.M., Umans, J.G., Howard, B.V., Sitlani, C.M., Siscovick, D.S., et al. (2018). Circulating sphingolipids, insulin, HOMA-IR, and HOMA-B: The Strong Heart Family Study. Diabetes 67, 1663-1672. https://doi.org/10.2337/ db17-1449.
- 24. Chaurasia, B., Tippetts, T.S., Mayoral Monibas, R., Liu, J., Li, Y., Wang, L., Wilkerson, J.L., Sweeney, C.R., Pereira, R.F., Sumida, D.H., et al. (2019). Targeting a ceramide double bond improves insulin resistance and hepatic steatosis. Science 365, 386-392. https://doi.org/10.1126/ science.aav3722.
- 25. Chaurasia, B., Kaddai, V.A., Lancaster, G.I., Henstridge, D.C., Sriram, S., Galam, D.L.A., Gopalan, V., Prakash, K.N.B., Velan, S.S., Bulchand, S., et al. (2016). Adipocyte ceramides regulate subcutaneous adipose browning, inflammation, and metabolism. Cell Metab. 24, 820-834. https://doi.org/10.1016/j.cmet.2016.10.002.
- 26. Xia, J.Y., Holland, W.L., Kusminski, C.M., Sun, K., Sharma, A.X., Pearson, M.J., Sifuentes, A.J., McDonald, J.G., Gordillo, R., and Scherer, P.E. (2015). Targeted induction of ceramide degradation leads to improved systemic metabolism and reduced hepatic steatosis. Cell Metab. 22, 266-278. https://doi.org/10.1016/j.cmet.2015.06.007.
- 27. Stankeviciute, G., Tang, P., Ashley, B., Chamberlain, J.D., Hansen, M.E. B., Coleman, A., D'Emilia, R., Fu, L., Mohan, E.C., Nguyen, H., et al. (2022). Convergent evolution of bacterial ceramide synthesis. Nat. Chem. Biol. 18, 305–312. https://doi.org/10.1038/s41589-021-00948-7.
- 28. Harrison, P.J., Dunn, T.M., and Campopiano, D.J. (2018). Sphingolipid biosynthesis in man and microbes. Nat. Prod. Rep. 35, 921-954. https://doi.org/10.1039/c8np00019k.
- 29. Johnson, E.L., Heaver, S.L., Waters, J.L., Kim, B.I., Bretin, A., Goodman, A.L., Gewirtz, A.T., Worgall, T.S., and Ley, R.E. (2020). Sphingolipids produced by gut bacteria enter host metabolic pathways impacting ceramide levels. Nat. Commun. 11, 2471. https://doi.org/10.1038/s41467-020-16274-w.
- 30. Brown, E.M., Ke, X., Hitchcock, D., Jeanfavre, S., Avila-Pacheco, J., Nakata, T., Arthur, T.D., Fornelos, N., Heim, C., Franzosa, E.A., et al. (2019). Bacteroides-derived sphingolipids are critical for maintaining intestinal homeostasis and symbiosis. Cell Host Microbe 25, 668-680. e7. https://doi.org/10.1016/j.chom.2019.04.002.
- 31. Le, H.H., Lee, M.T., Besler, K.R., and Johnson, E.L. (2022). Host hepatic metabolism is modulated by gut microbiota-derived sphingolipids. Cell Host Microbe 30, 798-808.e7. https://doi.org/10.1016/j.chom.2022. 05.002.
- 32. Lynch, J.B., Gonzalez, E.L., Choy, K., Faull, K.F., Jewell, T., Arellano, A., Liang, J., Yu, K.B., Paramo, J., and Hsiao, E.Y. (2023). Gut microbiota Turicibacter strains differentially modify bile acids and host lipids. Nat. Commun. 14, 3669. https://doi.org/10.1038/s41467-023-39403-7.
- 33. Maki, J.J., Nielsen, D.W., and Looft, T. (2020). Complete genome sequence and annotation for Turicibacter sanguinis MOL361T (DSM 14220). Microbiol. Resour. Announc. 9, e00475-20. https://doi.org/10. 1128/MRA.00475-20.
- 34. Santiago-Rodriguez, T.M., Fornaciari, G., Luciani, S., Dowd, S.E., Toranzos, G.A., Marota, I., and Cano, R.J. (2015). Gut microbiome of an 11th century A.D. Pre-Columbian Andean mummy. PLoS One 10, e0138135. https://doi.org/10.1371/journal.pone.0138135.
- 35. Albillos, A., de Gottardi, A., and Rescigno, M. (2020). The gut-liver axis in liver disease: Pathophysiological basis for therapy. J. Hepatol. 72, 558-577. https://doi.org/10.1016/j.jhep.2019.10.003.
- 36. Svegliati-Baroni, G., Patrício, B., Lioci, G., Macedo, M.P., and Gastaldelli, A. (2020). Gut-pancreas-liver axis as a target for treatment

Article



- of NAFLD/NASH. Int. J. Mol. Sci. 21, 5820. https://doi.org/10.3390/iims21165820.
- Martinez-Guryn, K., Hubert, N., Frazier, K., Urlass, S., Musch, M.W., Ojeda, P., Pierre, J.F., Miyoshi, J., Sontag, T.J., Cham, C.M., et al. (2018). Small intestine microbiota regulate host digestive and absorptive adaptive responses to dietary lipids. Cell Host Microbe 23, 458–469.e5. https://doi.org/10.1016/j.chom.2018.03.011.
- Chaurasia, B., and Summers, S.A. (2021). Ceramides in metabolism: key lipotoxic players. Annu. Rev. Physiol. 83, 303–330. https://doi.org/10. 1146/annurev-physiol-031620-093815.
- Poss, A.M., Maschek, J.A., Cox, J.E., Hauner, B.J., Hopkins, P.N., Hunt, S.C., Holland, W.L., Summers, S.A., and Playdon, M.C. (2020). Machine learning reveals serum sphingolipids as cholesterol-independent biomarkers of coronary artery disease. J. Clin. Invest. 130, 1363–1376. https://doi.org/10.1172/JCI131838.
- Kayser, B.D., Prifti, E., Lhomme, M., Belda, E., Dao, M.-C., Aron-Wisnewsky, J., Microobes Consortium, Kontush, A., Zucker, J.-D., Rizkalla, S.W., et al. (2019). Elevated serum ceramides are linked with obesity-associated gut dysbiosis and impaired glucose metabolism. Metabolomics 15, 140. https://doi.org/10.1007/s11306-019-1596-0.
- Li, Y., Chaurasia, B., Rahman, M.M., Kaddai, V., Maschek, J.A., Berg, J. A., Wilkerson, J.L., Mahmassani, Z.S., Cox, J., Wei, P., et al. (2023). Ceramides increase fatty acid utilization in intestinal progenitors to enhance stemness and increase tumor risk. Gastroenterology 165, 1136–1150. https://doi.org/10.1053/j.gastro.2023.07.017.
- Li, Y., Nicholson, R.J., and Summers, S.A. (2022). Ceramide signaling in the gut. Mol. Cell. Endocrinol. 544, 111554. https://doi.org/10.1016/j. mce.2022.111554.
- Choi, R.H., Tatum, S.M., Symons, J.D., Summers, S.A., and Holland, W.L. (2021). Ceramides and other sphingolipids as drivers of cardiovascular disease. Nat. Rev. Cardiol. 18, 701–711. https://doi.org/10.1038/ s41569-021-00536-1.
- 44. Fung, T.C., Vuong, H.E., Luna, C.D.G., Pronovost, G.N., Aleksandrova, A. A., Riley, N.G., Vavilina, A., McGinn, J., Rendon, T., Forrest, L.R., and Hsiao, E.Y. (2019). Intestinal serotonin and fluoxetine exposure modulate bacterial colonization in the gut. Nat. Microbiol. 4, 2064–2073. https://doi.org/10.1038/s41564-019-0540-4.
- Suez, J., Cohen, Y., Valdés-Mas, R., Mor, U., Dori-Bachash, M., Federici, S., Zmora, N., Leshem, A., Heinemann, M., Linevsky, R., et al. (2022). Personalized microbiome-driven effects of non-nutritive sweeteners on human glucose tolerance. Cell 185, 3307–3328.e19. https://doi.org/10. 1016/j.cell.2022.07.016.
- Dai, D., Zhu, J., Sun, C., Li, M., Liu, J., Wu, S., Ning, K., He, L.J., Zhao, X. M., and Chen, W.H. (2022). GMrepo v2: a curated human gut microbiome database with special focus on disease markers and cross-dataset comparison. Nucleic Acids Res. 50, D777–D784. https://doi.org/10.1093/nar/gkab1019.
- Golloso-Gubat, M.J., Ducarmon, Q.R., Tan, R.C.A., Zwittink, R.D., Kuijper, E.J., Nacis, J.S., and Santos, N.L.C. (2020). Gut microbiota and dietary intake of normal-weight and overweight Filipino children. Microorganisms 8, 1015. https://doi.org/10.3390/microorganisms8071015.
- Dhakal, S., McCormack, L., and Dey, M. (2020). Association of the gut microbiota with weight-loss response within a retail weight-management program. Microorganisms 8, 1246. https://doi.org/10.3390/microorganisms8081246.
- Wang, L., Wang, H., Zhang, B., Popkin, B.M., and Du, S. (2020). Elevated fat intake increases body weight and the risk of overweight and obesity among Chinese adults: 1991–2015 trends. Nutrients 12, 3272. https:// doi.org/10.3390/nu12113272.
- Vijay-Kumar, M., Aitken, J.D., Carvalho, F.A., Cullender, T.C., Mwangi, S., Srinivasan, S., Sitaraman, S.V., Knight, R., Ley, R.E., and Gewirtz, A.T. (2010). Metabolic syndrome and altered gut microbiota in mice lacking Toll-like receptor 5. Science 328, 228–231. https://doi.org/10.1126/ science.1179721.

- Le Chatelier, E., Nielsen, T., Qin, J., Prifti, E., Hildebrand, F., Falony, G., Almeida, M., Arumugam, M., Batto, J.M., Kennedy, S., et al. (2013). Richness of human gut microbiome correlates with metabolic markers. Nature 500, 541–546. https://doi.org/10.1038/nature12506.
- Velázquez, K.T., Enos, R.T., Bader, J.E., Sougiannis, A.T., Carson, M.S., Chatzistamou, I., Carson, J.A., Nagarkatti, P.S., Nagarkatti, M., and Murphy, E.A. (2019). Prolonged high-fat-diet feeding promotes non-alcoholic fatty liver disease and alters gut microbiota in mice. World J. Hepatol. 11, 619–637. https://doi.org/10.4254/wjh.v11.i8.619.
- 53. Research Diets Inc. (2025). Diet D12451: Rodent Diet With 45 kcal% Fat. https://researchdiets.com/formulas/d12451.
- Speakman, J.R. (2019). Use of high-fat diets to study rodent obesity as a model of human obesity. Int. J. Obes. (Lond.) 43, 1491–1492. https://doi. org/10.1038/s41366-019-0363-7.
- Brown, E.M., Clardy, J., and Xavier, R.J. (2023). Gut microbiome lipid metabolism and its impact on host physiology. Cell Host Microbe 31, 173–186. https://doi.org/10.1016/j.chom.2023.01.009.
- Frankfater, C.F., Sartorio, M.G., Valguarnera, E., Feldman, M.F., and Hsu, F.F. (2023). Lipidome of the Bacteroides genus containing new peptidolipid and sphingolipid families revealed by multiple-stage mass spectrometry. Biochemistry 62, 1160–1180. https://doi.org/10.1021/acs.biochem.2c00664.
- Miyamoto, J., Igarashi, M., Watanabe, K., Karaki, S.I., Mukouyama, H., Kishino, S., Li, X., Ichimura, A., Irie, J., Sugimoto, Y., et al. (2019). Gut microbiota confers host resistance to obesity by metabolizing dietary polyunsaturated fatty acids. Nat. Commun. 10, 4007. https://doi.org/10. 1038/s41467-019-11978-0.
- Simopoulos, A.P. (2016). An increase in the omega-6/omega-3 fatty acid ratio increases the risk for obesity. Nutrients 8, 128. https://doi.org/10. 3390/nu8030128.
- Kishino, S., Takeuchi, M., Park, S.B., Hirata, A., Kitamura, N., Kunisawa, J., Kiyono, H., Iwamoto, R., Isobe, Y., Arita, M., et al. (2013). Polyunsaturated fatty acid saturation by gut lactic acid bacteria affecting host lipid composition. Proc. Natl. Acad. Sci. USA. 110, 17808–17813. https://doi.org/10.1073/pnas.1312937110.
- Sanina, N., Chopenko, N., Mazeika, A., and Kostetsky, E. (2017). Nanoparticulate tubular immunostimulating complexes: novel formulation of effective adjuvants and antigen delivery systems. BioMed Res. Int. 2017, 4389525. https://doi.org/10.1155/2017/4389525.
- Fischer, S., Stegmann, F., Gnanapragassam, V.S., and Lepenies, B. (2022). From structure to function Ligand recognition by myeloid C-type lectin receptors. Comput. Struct. Biotechnol. J. 20, 5790–5812. https://doi.org/10.1016/j.csbj.2022.10.019.
- Lee, A.G. (2000). Membrane lipids: it's only a phase. Curr. Biol. 10, R377–R380. https://doi.org/10.1016/s0960-9822(00)00477-2.
- Yu, C.W., Lin, Y.T., and Li, H.M. (2020). Increased ratio of galactolipid MGDG: DGDG induces jasmonic acid overproduction and changes chloroplast shape. New Phytol. 228, 1327–1335. https://doi.org/10.1111/nph.16766.
- Zhang, F., Chen, Z., Jiang, L., Chen, Z., and Sun, H. (2021). Response of fecal bacterial flora to the exposure of fumonisin B1 in BALB/c mice. Toxins (Basel) 13, 612. https://doi.org/10.3390/toxins13090612.
- Lee, M.T., Le, H.H., and Johnson, E.L. (2021). Dietary sphinganine is selectively assimilated by members of the mammalian gut microbiome.
 J. Lipid Res. 62, 100034. https://doi.org/10.1194/jlr.RA120000950.
- Molenaar, M.R., Jeucken, A., Wassenaar, T.A., van de Lest, C.H.A., Brouwers, J.F., and Helms, J.B. (2019). LION/web: a web-based ontology enrichment tool for lipidomic data analysis. GigaScience 8, giz061. https://doi.org/10.1093/gigascience/giz061.
- Molenaar, M.R., Haaker, M.W., Vaandrager, A.B., Houweling, M., and Helms, J.B. (2023). Lipidomic profiling of rat hepatic stellate cells during activation reveals a two-stage process accompanied by increased levels of lysosomal lipids. J. Biol. Chem. 299, 103042. https://doi.org/10.1016/j. jbc.2023.103042.



- 68. Wahlström, A., Sayin, S.I., Marschall, H.U., and Bäckhed, F. (2016). Intestinal crosstalk between bile acids and microbiota and its impact on host metabolism. Cell Metab. 24, 41-50. https://doi.org/10.1016/j. cmet.2016.05.005.
- 69. Li, X., Shimizu, Y., and Kimura, I. (2017). Gut microbial metabolite shortchain fatty acids and obesity. Biosci. Microbiota Food Health 36, 135-140. https://doi.org/10.12938/bmfh.17-010.
- 70. Sze, M.A., and Schloss, P.D. (2016). Looking for a signal in the noise: revisiting obesity and the microbiome. mBio 7, e01018-16. https://doi.org/ 10.1128/mBio.01018-16.
- 71. Guan, Z.W., Yu, E.Z., and Feng, Q. (2021). Soluble dietary fiber, one of the most important nutrients for the gut microbiota. Molecules 26, 6802. https://doi.org/10.3390/molecules26226802.
- 72. Makki, K., Deehan, E.C., Walter, J., and Bäckhed, F. (2018). The impact of dietary fiber on gut microbiota in host health and disease. Cell Host Microbe 23, 705-715. https://doi.org/10.1016/j.chom.2018.05.012.
- 73. Wu, G., Tang, X., Fan, C., Wang, L., Shen, W., Ren, S., Zhang, L., and Zhang, Y. (2021). Gastrointestinal tract and dietary fiber driven alterations of gut microbiota and metabolites in Durco × Bamei crossbred pigs. Front. Nutr. 8, 806646. https://doi.org/10.3389/fnut.2021.806646.
- 74. Sonnenburg, E.D., and Sonnenburg, J.L. (2014). Starving our microbial self: the deleterious consequences of a diet deficient in microbiotaaccessible carbohydrates. Cell Metab. 20, 779-786. https://doi.org/10. 1016/j.cmet.2014.07.003.
- 75. Peng, Z., and Miao, X. (2020). Monoglucosyldiacylglycerol participates in phosphate stress adaptation in Synechococcus sp. PCC 7942. Biochem. Biophys. Res. Commun. 522, 662-668. https://doi.org/10.1016/j.bbrc. 2019.11.143.
- 76. Jiao, N., Baker, S.S., Nugent, C.A., Tsompana, M., Cai, L., Wang, Y., Buck, M.J., Genco, R.J., Baker, R.D., Zhu, R., and Zhu, L. (2018). Gut microbiome may contribute to insulin resistance and systemic inflammation in obese rodents: a meta-analysis. Physiol. Genomics 50, 244-254. https://doi.org/10.1152/physiolgenomics.00114.2017.
- 77. Li, T.T., Tong, A.J., Liu, Y.Y., Huang, Z.R., Wan, X.Z., Pan, Y.Y., Jia, R.B., Liu, B., Chen, X.H., and Zhao, C. (2019). Polyunsaturated fatty acids from microalgae Spirulina platensis modulates lipid metabolism disorders and gut microbiota in high-fat diet rats. Food Chem. Toxicol. 131, 110558. https://doi.org/10.1016/j.fct.2019.06.005.
- 78. Liu, W., Crott, J.W., Lyu, L., Pfalzer, A.C., Li, J., Choi, S.W., Yang, Y., Mason, J.B., and Liu, Z. (2016). Diet- and genetically-induced obesity produces alterations in the microbiome, inflammation and Wnt pathway in the intestine of Apc+/1638N mice: comparisons and contrasts. J. Cancer 7, 1780-1790. https://doi.org/10.7150/jca.15792.
- 79. Jin, M., Li, J., Liu, F., Lyu, N., Wang, K., Wang, L., Liang, S., Tao, H., Zhu, B., and Alkasir, R. (2019). Analysis of the gut microflora in patients with Parkinson's disease. Front. Neurosci. 13, 1184. https://doi.org/10. 3389/fnins.2019.01184.
- 80. Barandouzi, Z.A., Starkweather, A.R., Henderson, W.A., Gyamfi, A., and Cong, X.S. (2020). Altered composition of gut microbiota in depression: a systematic review. Front. Psychiatry 11, 541. https://doi.org/10.3389/ fpsvt.2020.00541.
- 81. Love, M.I., Huber, W., and Anders, S. (2014). Moderated estimation of fold change and dispersion for RNA-seq data with DESeq2. Genome Biol. 15, 550. https://doi.org/10.1186/s13059-014-0550-8.
- 82. de Jong, A., Kuipers, O.P., and Kok, J. (2022). FUNAGE-Pro: comprehensive web server for gene set enrichment analysis of prokaryotes. Nucleic Acids Res. 50, W330-W336. https://doi.org/10.1093/nar/gkac441.
- 83. Browne, H.P., Forster, S.C., Anonye, B.O., Kumar, N., Neville, B.A., Stares, M.D., Goulding, D., and Lawley, T.D. (2016). Culturing of 'unculturable' human microbiota reveals novel taxa and extensive sporulation. Nature 533, 543-546. https://doi.org/10.1038/nature17645.
- 84. Pruesse, E., Peplies, J., and Glöckner, F.O. (2012). SINA: accurate highthroughput multiple sequence alignment of ribosomal RNA genes.

- Bioinformatics 28, 1823-1829. https://doi.org/10.1093/bioinformatics/
- 85. Rey, F.E., Gonzalez, M.D., Cheng, J., Wu, M., Ahern, P.P., and Gordon, J. I. (2013). Metabolic niche of a prominent sulfate-reducing human gut bacterium. Proc. Natl. Acad. Sci. USA. 110, 13582-13587. https://doi. org/10.1073/pnas.1312524110.
- 86. Matyash, V., Liebisch, G., Kurzchalia, T.V., Shevchenko, A., and Schwudke, D. (2008). Lipid extraction by methyl-tert-butyl ether for high-throughput lipidomics. J. Lipid Res. 49, 1137-1146. https://doi. org/10.1194/jlr.D700041-JLR200.
- 87. Alshehry, Z.H., Barlow, C.K., Weir, J.M., Zhou, Y., McConville, M.J., and Meikle, P.J. (2015). An efficient single phase method for the extraction of plasma lipids. Metabolites 5, 389-403. https://doi.org/10.3390/ metabo5020389.
- 88. Koelmel, J.P., Kroeger, N.M., Ulmer, C.Z., Bowden, J.A., Patterson, R.E., Cochran, J.A., Beecher, C.W.W., Garrett, T.J., and Yost, R.A. (2017). LipidMatch: an automated workflow for rule-based lipid identification using untargeted high-resolution tandem mass spectrometry data. BMC Bioinform. 18, 331. https://doi.org/10.1186/s12859-017-1744-3.
- 89. Stappenbeck, T.S., Hooper, L.V., Manchester, J.K., Wong, M.H., and Gordon, J.I. (2002). Laser capture microdissection of mouse intestine: characterizing mRNA and protein expression, and profiling intermediary metabolism in specified cell populations. Methods Enzymol. 356, 167-196. https://doi.org/10.1016/s0076-6879(02)56932-9.
- 90. Subramanian, A., Tamayo, P., Mootha, V.K., Mukherjee, S., Ebert, B.L., Gillette, M.A., Paulovich, A., Pomeroy, S.L., Golub, T.R., Lander, E.S., and Mesirov, J.P. (2005). Gene set enrichment analysis: a knowledgebased approach for interpreting genome-wide expression profiles. Proc. Natl. Acad. Sci. USA. 102, 15545-15550. https://doi.org/10. 1073/pnas.0506580102.
- 91. Mootha, V.K., Lindgren, C.M., Eriksson, K.F., Subramanian, A., Sihag, S., Lehar, J., Puigserver, P., Carlsson, E., Ridderstråle, M., Laurila, E., et al. (2003). PGC-1alpha-responsive genes involved in oxidative phosphorylation are coordinately downregulated in human diabetes. Nat. Genet. 34, 267-273. https://doi.org/10.1038/ng1180.
- 92. Chen, S., Zhou, Y., Chen, Y., and Gu, J. (2018). fastp: an ultra-fast all-inone FASTQ preprocessor. Bioinformatics 34, i884-i890. https://doi.org/ 10.1093/bioinformatics/btv560.
- 93. Kim, D., Paggi, J.M., Park, C., Bennett, C., and Salzberg, S.L. (2019). Graph-based genome alignment and genotyping with HISAT2 and HISAT-genotype. Nat. Biotechnol. 37, 907-915. https://doi.org/10. 1038/s41587-019-0201-4.
- 94. Danecek, P., Bonfield, J.K., Liddle, J., Marshall, J., Ohan, V., Pollard, M.O., Whitwham, A., Keane, T., McCarthy, S.A., Davies, R.M., and Li, H. (2021). Twelve years of SAMtools and BCFtools. GigaScience 10, giab008. https://doi.org/10.1093/gigascience/giab008.
- 95. Chung, M., Adkins, R.S., Mattick, J.S.A., Bradwell, K.R., Shetty, A.C., Sadzewicz, L., Tallon, L.J., Fraser, C.M., Rasko, D.A., Mahurkar, A., and Dunning Hotopp, J.C. (2021). FADU: a quantification tool for prokaryotic transcriptomic analyses. mSystems 6, e00917-20. https://doi.org/ 10.1128/mSystems.00917-20.
- 96. Love, M.I., Soneson, C., Hickey, P.F., Johnson, L.K., Pierce, N.T., Shepherd, L., Morgan, M., and Patro, R. (2020). Tximeta: Reference sequence checksums for provenance identification in RNA-seq. PLoS Comput. Biol. 16, e1007664. https://doi.org/10.1371/journal.pcbi. 1007664.
- 97. Stephens, M. (2017). False discovery rates: a new deal. Biostatistics 18, 275-294. https://doi.org/10.1093/biostatistics/kxw041.
- 98. Gu. Z. (2022). Complex heatmap visualization, Imeta 1, e43, https://doi. org/10.1002/imt2.43.
- 99. Geiger, O., González-Silva, N., López-Lara, I.M., and Sohlenkamp, C. (2010). Amino acid-containing membrane lipids in bacteria. Prog. Lipid Res. 49, 46-60. https://doi.org/10.1016/j.plipres.2009.08.002.

Cell Metabolism

Article



- Katoh, K., and Standley, D.M. (2014). MAFFT: iterative refinement and additional methods. Methods Mol. Biol. 1079, 131–146. https://doi.org/ 10.1007/978-1-62703-646-7_8.
- 101. Kanehisa, M., Sato, Y., and Morishima, K. (2016). BlastKOALA and GhostKOALA: KEGG tools for functional characterization of genome and metagenome sequences. J. Mol. Biol. 428, 726–731. https://doi. org/10.1016/j.jmb.2015.11.006.
- Di Tommaso, P., Chatzou, M., Floden, E.W., Barja, P.P., Palumbo, E., and Notredame, C. (2017). Nextflow enables reproducible computational workflows. Nat. Biotechnol. 35, 316–319. https://doi.org/10.1038/ nbt.3820.
- Breitwieser, F.P., and Salzberg, S.L. (2020). Pavian: interactive analysis of metagenomics data for microbiome studies and pathogen identification. Bioinformatics 36, 1303–1304. https://doi.org/10.1093/bioinformatics/btz715.



Cell MetabolismArticle

STAR*METHODS

KEY RESOURCES TABLE

REAGENT or RESOURCE	SOURCE	IDENTIFIER
Bacterial and virus strains		
Bacteroides uniformis	ATCC	ATCC 8492
Desulfovibrio desulfuricans subsp. desulfuricans	ATCC	ATCC 27774
Escherichia coli Nissle 1917	Gift from Matt Mulvey	N/A
Turicibacter sp.	Round lab strain	JLR.KK008
Chemicals, peptides, and recombinant proteins		
Alkyne Sphinganine	Click Chemistry Tools	Cat# 1452-1
Ceramide LIPIDOMIX	Avanti Research	Cat# 330712
DNA/RNA shield	Zymo Research	Cat# R1100-50
EquiSPLASH LIPIDOMIX	Avanti Research	Cat# 330731
Fenretinide	Cayman Chemical	Cat# 17688
Fumonisin B1	Sigma-Aldrich	Cat# SML1286
Myriocin	Sigma-Aldrich	Cat# M1177-25MG
NEBNext rRNA Depletion Solution (bacteria)	NEB	Cat# E7850L
OCT	Fisher	Cat# 23-730.571
Palmitic acid	Sigma-Aldrich	Cat# P5585
Palmitic acid alkyne	Cayman Chemical	Cat# 13266
qScriptc DNA SuperMix	QuantaBio	Cat#101414-106
Scheadlers broth	Thermo Scientific	Cat# CM0497B
SM LIPIDOMIX	Avanti Research	Cat# 330707
YCFA Agar	Anaerobe Systems	Cat# AS-675
YCFA Broth	Anaerobe Systems	Cat# AS-680
Critical commercial assays		
Agilent Technologies 2200 TapeStation	Agilent Technologies	Cat# 5067-5582
Click-iT Plus Alexa Fluor 647 Picolyl Azide Toolkit	Thermo Scientific	Cat# C10643
D1000 ScreenTape assay	Agilent Technologies	Cat# 5067-5583
Direct-zol RNA MiniPrep Kit	Zymoresearch	Cat# R2050
HostZERO microbial DNA kit;	ZymoResearch	Cat# D4310
Infinity triglycerides reagent	Thermo Scientific	Cat# TR22421
Insulin ELISA kit	Crystal Chem	Cat# 90080
Kapa Biosystems Kapa Library Quant Kit	Sigma	Cat# KK4824
NEBNext Ultra II RNA Library Prep Kit for Illumina	NEB	Cat# E7770L
Nextera DNA Flex Library Prep kit	Illumina	Cat# 20025520
PowerFecal Pro	Qiagen	Cat# 51804
Purelink Microbiome DNA purification kit	Invitrogen	Cat# A29790
QBT Fatty Acid Uptake Assay Kit	Molecular Devices	Cat# R8132
RNeasy micro kit	Qiagen	Cat# 74004
Deposited data	<u> </u>	
SF community metagenomic sequences	N/A	PRJNA1137940
RNAseq data small intestine	N/A	PRJNA1122642 and GEO GSE269607
Turicibacter culture RNAseq	N/A	PRJNA1135257
Turicibacter KK03	N/A	PRJNA1061597
Experimental models: Cell lines		-
MODE-K cells	Round Lab	RRID:CVCL_B4FG

Cell Metabolism

Article



Continued		
REAGENT or RESOURCE	SOURCE	IDENTIFIER
Experimental models: Organisms/strains		
Myd88LoxP/LoxP; CD4-Cre+.B6	Taconic/Round Lab	N/A
Wild-type mice (C57BL/6)	Round lab, from JAX	N/A
Oligonucleotides		
See Table S5	N/A	N/A
Software and algorithms		
Biorender	https://biorender.com	N/A
DESeq2	Love et al. ⁸¹	N/A
FACoP.v2 FUNAGE-Pro software	de Jong et al. ⁸²	N/A
FlowJo	FlowJo LLC	N/A
GSEA	https://www.gsea-msigdb.org/	N/A
GraphPad Prism GraphPad Software	N/A	Version 10
HMMER v. 3.3.2	http://hmmer.org	N/A
HiSat2 (v2.1.0)	https://genome.cshlp.org/ content/31/7/1290.abstract	N/A
IMG/M	https://img.jgi.doe.gov/	N/A
LION/web	www.lipidontology.com	N/A
MassHunter software	Agilent	N/A
MetaboAnalyst	https://www.metaboanalyst.ca/	v 6.0
Other		
45 kcal% fat DIO mouse feed	Research Diets	Cat# D12451
Contour Next EZ Glucose Meter	Bayer	Cat# B009AVO7PE
Contour Next Test Strips	Bayer	Cat# B014JZJEU8
Vinyl Anaerobic Chambers	Coy Lab Products	Cat# 7150000

EXPERIMENTAL MODEL AND SUBJECT DETAILS

Mice

C57Bl/6 Myd88LoxP/LoxP mice (Jackson Laboratories) were crossed to C57Bl/6 CD4-Cre mice (Taconic) to produce Myd88+/+; CD4-Cre+ mice (WT) and Myd88LoxP/LoxP; CD4-Cre+ (T-Myd88-/-) mice. Age-matched 8-10-week-old male mice were used to compare the weight phenotype on HFD. 6-week-old WT C57Bl/6 mice (Jackson Laboratories) mice from our facility were used to compare the weight phenotype on a HFD. GF C57Bl/6 mice were used and maintained in sterile isolators and verified monthly for GF status by plating and PCR of feces. The use of mice in all experiments was in strict adherence to federal regulations as well as the guidelines for animal use set forth by the University of Utah Institutional Animal Care and Use Committee Protocol #00001562.

METHOD DETAILS

Colonization of mice with spore-forming microbes

Fecal pellets were taken from WT mice and incubated in reduced PBS containing 3% chloroform (v/v) for 1 hour at 37 $^{\circ}$ C in an anaerobic chamber. After incubation, tubes were gently mixed, and fecal material was allowed to settle for 10 sec. Supernatant was transferred to a fresh tube and chloroform was removed by forcing CO₂ into the tube.

For spore-forming associations with germfree mice, tubes containing gavage material were sterilized in the port of a germfree isolator for 1 hour before pulling them into the isolator for gavage. Breeder pairs were then orally gavaged with 200 uL of the spore-forming cocktail. Their offspring were sacrificed at 8 weeks of age for analysis of the small intestine and serum. For spore-forming (SF) experiments in conventional conditions, mice treated with the SF community were orally gavaged with 200 uL of intestinal contents from the SF colonized mice resuspended in reduced PBS containing 0.1% cystine at a concentration of 100mg/mL five days a week.

Culture Collection and Turicibacter Isolation

Luminal contents from the intestines (cecum, small, and large intestine) of SF colonized mice were harvested and placed in anaerobic conditions within 1 h of passing to preserve the viability of anaerobic bacteria. All sample processing and culturing took place under



anaerobic conditions at 37 °C. Culture media, PBS and all other materials that were used for culturing were placed in the anaerobic chamber 24 h before use to reduce to anaerobic conditions (Coy Lab Products, Vinyl Anaerobic Chambers, Cat # 7150000). Samples were homogenized in reduced PBS+ 0.1% cysteine (100mg luminal contents/mL PBS), then serially diluted and plated directly onto YCFA agar supplemented with 0.002 g/ml each of glucose, maltose, and cellobiose in large (13.5 cm diameter) Petri dishes. ⁸³ For the isolation of *Turicibacter*, the luminal contents from the SF colonized mice were treated with 3% chloroform (v/v) for 1 hour at 37 °C in an anaerobic chamber, and then it was serial diluted and plated on YCFA. Individual colonies were picked after 48 hours, streaked to isolation, liquid cultures were started from individual colonies in YFCA, and DNA was extracted using Purelink Microbiome DNA purification kit (Invitrogen). Identification of each isolate was performed by PCR amplification of the full-length 16S rRNA gene using S-D-Bact-0008-a-S-16 (GM3_F): AGAGTTTGATCMTGGC forward primer and S-D-Bact-1492-a-A-16 (GM4_R): TACCTTGTTACGACTT reverse primer followed by capillary sequencing. Full-length 16S rRNA gene sequence reads were aligned in the Silva to assign taxonomic designations to the genus level. ⁸⁴

Monocolonization experiments

At weaning GF WT mice were gavaged with pure cultures from the SF culture collections and housed in sterile conditions for eight weeks.

Turicibacter Culturing

For gavaging experiments *Turicibacter* was isolated as described above. For gavaging SPF animals with *Turicibacter* cultures, *Turicibacter* was grown overnight in Scheadlers broth (Thermo Scientific CM0497B). For every 5 mice to be gavaged 10mL of culture was grown to an OD of 0.5 600nm, spun down at 5000rpm for 10min, all supernatant was removed and the bacteria was resuspended in 1.5mL of reduced PBS +0.1% cystine from the anaerobic chamber. Immediately 200uL of the *Turicibacter* sample or PBS +0.1% cystine vehicle control was gavaged into mice five times a week.

For the growth of *Turicibacter* in PA (Palmitic acid Sigma-Aldrich P5585), PA was dissolved in ethanol and added to *Turicibacter* cultures.

Bacterial growth and uptake of PA

To test how different bacteria grow in and take up PA, we used 25 or 5 μM palmitic acid alkyne (PAA, Cayman Chemical), or palmitic acid (Sigma-Aldrich). The following bacteria were used: *Bacteroides uniformis* strain JCM5828 (ATCC 8492) grown under anaerobic conditions at 37 °C in Scheadlers, *E. coli Nissle* 1917 (gift from Matt Mulvey) grown under aerobic conditions at 37 °C in Scheadlers, and *Desulfovibrio desulfuricans* ATCC (#27774) was grown under anaerobic conditions at 37 °C in *Desulfovibrio* media described previously. ⁸⁵ *Desulfovibrio* media was composed of NH4Cl (1 g/L) (Fisher Chemical), Na2SO4 (2 g/L) (Fisher Chemical), Na2S2O3·5H2O (1 g/L) (Sigma), MgSO4·7H2O(1 g/L) (Fisher Chemical), CaCl2·2H2O (0.1 g/L) (Fisher Chemical), KH2PO4 (0.5 g/L) (Fisher Bioreagents), Yeast Extract (1 g/L) (Amresco), Resazurin (0.5 mL/L) (Sigma), cysteine (0.6 g/L) (Sigma), DTT (0.6 g/L) (Sigma), NaHCO3 (1 g/L) (Fisher Chemical), pyruvic acid (3 g/L) (Acros Organics), malic acid (3 g/L) (Acros Organics), ATCC Trace Mineral Mix (10 mL/L), ATCC VitaminMix (10 mL/L) and adjusted to pH of 7.2. After 24 hours of incubation, the cultures were harvested by centrifugation at 18,000 g for 10 min. at room temperature. Cell pellets were washed with PBS and then washed three times with 1% FBS/PBS. Washed cell pellets were then fixed with 4% paraformaldehyde in PBS for labeling with fluorophore Alexa Fluor 647 azide (AF647-azide; Invitrogen, Carlsbad, CA). Samples were then washed once, resuspended in 1% FBS/PBS, and then run on BD LSR Fortessa and analyzed with FlowJo software.

Diet treatment

Mice housed within the SPF facility were fed a standard chow of irradiated 2920x (Envigo). Mice were fed a high fat diet of 45 kcal% fat DIO mouse feed (Research Diets D12451)

Metabolic phenotyping

Total body fat composition was measured on an NMR Bruker Minispec.

Blood Glucose measurement

Mice were fasted for 12 hours overnight prior to blood glucose measurements glucose. Fasting levels of glucose were detected using a Contour Glucose Meter (Bayer) and Contour Glucose Strips (Bayer).

Insulin ELISA

Serum was collected from 6-hour-fasted mice, and insulin was measured using a mouse insulin enzyme-linked immunosorbent assay (ELISA) kit (Crystal Chem). Serum samples were run in duplicate according to the manufacturer's instructions.

Triglyceride assay

Serum from mice fasted for 12 hours was used with the infinity triglycerides reagent (Thermo Scientific TR22421) according to the manufacturer's instructions.

Cell Metabolism

Article



GMrepo

The data repository for human gut microbiota (https://gmrepo.humangut.info/home) was searched for the *Turicibacter* NCBI taxonomic ID (191303), and the reads for *Turicibacter* with the human phenotypes of Health and Obesity were accessed. 46

Turicibacter lipid extraction for gavaging

A *Turicibacter* culture of 500mL was grown overnight in Scheadlers media to an OD600nm of 0.5. The culture was aliquoted into 50 10mL portions, spun down, resuspended in 300μ L PBS, and sonicated for 10 seconds at 30% (probe sonicator). 288uL of *Turicibacter* KKT8 homogenate was mixed with 345μ L methanol, 1149uL MTBE (methyl tert-butyl ether). The samples were then incubated for 60 min on ice with brief vortexing every 15 min. Following centrifugation for phase separation, the upper phase was transferred to another Eppendorf tube, which was dried using a Speedvac. Samples were stored at -80 °C until ready for use, upon which they were resuspended 1.5mL in 50% PEG-400, 0.5% Tween 80, and 49.5% distilled water. Mice were gavaged five days a week with 200μ L *Turicibacter* KKT8 lipids or vehicle.

In vitro experiments using mouse intestinal epithelial cells (MODE-K cells)

Mouse intestinal epithelial cells were maintained in Dulbecco's modified Eagle's medium (DMEM), with 2 mM L-glutamine and 1 mM sodium pyruvate. DMEM was supplemented with 10% FBS, 1% (v/v) glutamine, penicillin–streptomycin, and 1% HEPES.

MODE-K cell co-incubation with *Turicibacter*

To assess the effects of metabolite transfer from Turicibacter KKT8 to intestinal epithelial cells, MODE-K cells were incubated with Turicibacter KKT8 in tissue culture dishes (Corning Inc.), wherein bacterial cells were placed directly into the well or on a $0.4~\mu$ M filter situated 1mm above the monolayer of MODE-K cells. Turicibacter KKT8 cultures (OD600 of 0.20) were grown overnight in Scheadlers media supplemented with 25μ M palmitic acid alkyne (PAA, Cayman Chemical), then washed once in PBS and resuspended in 6 mL of 10% FBS in DMEM. 25% of the well volume of the PAA labeled Turicibacter KKT8 was added to the well directly or the transwell insert in 24-well plates. MODE-K cells were collected 4 hours after the addition of the bacteria. Alkyne-containing metabolites in bacterial and MODE-K cells were labeled with Alexa Fluor 647 azide using the Click iT cell reaction buffer kit (Thermo Fisher Scientific). Samples were then washed once, resuspended in 1% FBS/PBS, and then run on BD LSR Fortessa and analyzed with FlowJo software.

Fatty Acid Uptake Assay

MODE-K cells were seeded at 70,000 cells/well in 96 well plates (Corning 353219) and grown overnight. The following day cells were treated with 25% of the well volume of Scheadlers media, *Turicibacter* KKT8 resuspended in PBS to an OD600nm of 0.5, 1% Ethanol or 1% *Turicibacter* KKT8 lipids resuspended in 150uL of EtOH and incubated overnight. The next morning, all media was removed and replaced with serum-free media for 1 hour before the fatty acid uptake was performed. Fatty acid uptake was monitored using a QBT Fatty Acid Uptake Assay Kit (Molecular Devices). BODIPY-dodecanoic acid fluorescent fatty acid analog was added (QBTTM Fatty Acid Uptake Assay Kit, Molecular Devices) and the plate was immediately transferred to a fluorescence microplate reader for kinetic reading (every 20 seconds for 30-60 minutes) using a bottom-read mode. Measurement was done with an excitation filter of 480 nm and an emission filter of 520.

RNA isolation from small intestine for qPCR

Tissue sections 0.5 cm in length or 1×105 cells were stored at -70 °C in 700 mL of RiboZol (VWR). RNA was isolated using the Direct-zol RNA MiniPrep Kit (Zymoresearch). cDNA was synthesized using qScript cDNA synthesis kit (Quanta Biosciences). qPCR was conducted using LightCycler 480 SYBR Green I Master (Roche). qPCR experiments were conducted on a LightCycler LC480 instrument (Roche).

Lipidomics

Lipidomics analyses were performed at the University of Utah Metabolomics Core Facility using semi-quantitative LC-MS/MS platforms. Analyses were conducted across multiple sample types, including serum, cultured cells, and bacteria, using previously described protocols with modifications as noted below.^{86,87}

Lipidomics Chemicals

LC-MS-grade methanol, acetonitrile, isopropanol, and formic acid were obtained from Honeywell Burdick & Jackson (Morristown, NJ); methyl tert-butyl ether (MTBE) from Fisher Scientific (Waltham, MA); and ammonium formate and ammonium acetate from Sigma-Aldrich/Fluka (St. Louis, MO). Internal standards were obtained from Avanti Polar Lipids (Alabaster, AL) and included EquiSPLASH LIPIDOMIX (330731), SM LIPIDOMIX (330707), Ceramide LIPIDOMIX (330712), C18:1 dihydroceramide (d18:0/18:1 (9Z); 5 pmol/sample), C17-glucosylceramide (50 pmol/sample), TG(15:0_18:1(d7)_15:0) (492 pmol/sample), DG(15:0_18:1(d7)) (500 pmol/sample), PC(15:0_18:1(d7)) (500 pmol/sample), sphingosine-d7 (5 pmol/sample), S1P(d18:1-d7) (3 pmol/sample), and Sa1P(d18:0(d7)) (3 pmol/sample).

Lipidomics Sample Preparation

Serum samples were extracted using a modified butanol:methanol (1:1, v/v) protocol adapted from Alshehry et al. ⁸⁷ Briefly, samples were diluted at a 1:10 (v/v) sample-to-solvent ratio in the presence of internal standards, sonicated for 10 min on ice, vortexed, and





further sonicated for 1 h at 20 ± 5 °C. Following centrifugation at $13,000 \times g$ for 10 min at 4 °C, the supernatant was transferred to LC-MS vials. For cells and bacterial samples (e.g., SID, MODE-K, Turicibacter), $100 \, \mu L$ of homogenate (from $120 \, \mu L$ PBS) was transferred to tubes with $225 \, \mu L$ methanol containing internal standards, followed by the addition of $750 \, \mu L$ MTBE. After vortexing and incubation on ice for 1 h, samples were centrifuged to induce phase separation. The upper organic layer was transferred and dried under vacuum prior to LC-MS analysis. A $20 \, \mu L$ aliquot of the initial homogenate was saved for protein quantification (BCA assay, Thermo Fisher).

Lipidomics LC-MS Analysis

All lipid extracts were analyzed using UPLC coupled to either triple quadrupole (QQQ) or quadrupole time-of-flight (QTOF) instruments, depending on sample type and analysis goals. Chromatographic separation was performed on an Acquity UPLC CSH C18 column ($2.1 \times 100 \text{ mm}$, $1.7 \mu \text{m}$) with a VanGuard pre-column ($2.1 \times 5 \text{ mm}$, $1.7 \mu \text{m}$) maintained at 65 °C. Samples were randomized for injection with pooled quality control (QC) samples interspersed (n = 8 per run).

For targeted lipidomics (SID and MODE-K samples), analyses were conducted on an Agilent 6490 QQQ MS operated in positive-ion dynamic MRM (dMRM) mode. Mobile phase A was ACN:H₂O (60:40) with 10 mM ammonium formate and 0.1% formic acid; mobile phase B was IPA:ACN:H₂O (90:9:1) with identical modifiers. The gradient started at 15% B and ramped to 99% B by 7.14 min, held until 9.45 min, then re-equilibrated (total runtime: 13.3 min; flow rate: 0.4 mL/min). The injection volume was 3 μ L. Instrument parameters included a gas temperature of 175 °C, 15 L/min gas flow, and a capillary voltage of 3500 V. Collision energies and transitions were optimized using class-specific lipid standards. Phosphatidylcholines and sphingomyelins were monitored at m/z 184.1; ceramides at m/z 264.2 or 271.3 (labeled); dihydroceramides at m/z 284.3; and glycerolipids via [M+NH₄]+ with neutral loss. For untargeted lipidomics (*Turicibacter* samples), analysis was performed on an Agilent 6545 QTOF in positive and negative modes. Chromatographic and mobile phase conditions were similar, with ammonium acetate replacing ammonium formate in negative mode. Data were acquired over m/z 100–1700 with iterative MS/MS using collision energies of 20 V (positive) and 27.5 V (negative). Injection volumes were 2 μ L (positive) and 8 μ L (negative). Source conditions were optimized per mode (e.g., 225–300 °C gas temp, 11 L/min flow, 3500 V capillary voltage).

Lipidomics Data Processing and Quantification

Raw files were processed using Agilent MassHunter software (Qualitative and Quantitative packages). For both targeted and untargeted workflows, lipids were filtered for inclusion based on two criteria: (1) relative standard deviation (RSD) <30% in pooled QC samples, and (2) background signal <30% of QC signal in process blanks. Lipid abundances were normalized to class-specific internal standards and then to sample input (volume or protein content). For untargeted analysis, lipid annotation was performed using accurate mass and MS/MS spectral matching against the LipidMatch database, ⁸⁸ followed by manual validation. Positive and negative ion mode results were merged by lipid class.

Lipidomics Statistical Analysis and Visualization

Normalized lipid values were log_{10} -transformed and Pareto-scaled prior to univariate and multivariate analysis. Volcano plots, PCA, and heatmaps were generated in MetaboAnalyst. Significance thresholds were set at fold-change >1.5 and adjusted p < 0.05 (FDR-corrected). Additional figures were generated using Prism 10 (GraphPad Software). 16199517

Lipidomics LION Analysis

LION/web is a powerful online tool for lipid ontology enrichment analysis. It is a web-based interface (www.lipidontology.com) utilizes the LION (lipid ontology) database, which associates over 50,000 lipid species with biophysical, chemical, and cell biological features. Using the "ranking" mode for enrichment analysis Lipid abundances were uploaded in a CVS format and the performed enrichment analysis using Fisher's exact test or Kolmogorov-Smirnov test, depending on the chosen mode. The results are presented as enriched LION-terms with corresponding *p-values* and FDR-corrected *q-values*. ^{66,67}

Full List of Targeted Lipid MRM Transitions and Retention Times

target	transition	RT (min)	Internal Standard
Cer 18:0;O2/16:0	540.5 -> 284.3	4.9	Cer 18:0;O2/18:1
Cer 18:0;O2/18:0	568.6 -> 284.3	5.5	Cer 18:0;O2/18:1
Cer 18:0;O2/18:1	566.6 -> 284.3	4.9	internal standard
Cer 18:0;O2/20:0	596.6 -> 284.4	6.1	Cer 18:0;O2/18:1
Cer 18:0;O2/22:0	624.6 -> 284.4	6.7	Cer 18:0;O2/18:1
Cer 18:0;O2/24:0	652.7 -> 284.4	7.3	Cer 18:0;O2/18:1
Cer 18:0;O2/24:1	650.7 -> 284.3	6.6	Cer 18:0;O2/18:1
·			

Article



Continued			
target	transition	RT (min)	Internal Standard
Cer 18:1;O2/16:0	538.5 -> 264.2	4.7	Cer 18:1;O2/16:0[M[2]H7]
er 18:1;O2/18:0	566.6 -> 264.2	5.3	Cer 18:1;O2/18:0[M[2]H7]
Cer 18:1;O2/20:0	594.6 -> 264.2	5.8	Cer 18:1;O2/18:0[M[2]H7]
Cer 18:1;O2/22:0	622.6 -> 264.2	6.5	Cer 18:1;O2/24:1[M[2]H7]
Cer 18:1;O2/24:0	650.6 -> 264.2	7.0	Cer 18:1;O2/24:0[M[2]H7]
Ser 18:1;O2/24:1	648.6 -> 264.2	6.4	Cer 18:1;O2/24:1[M[2]H7]
Cer 18:1;O2/26:0	678.6 -> 264.2	7.6	Cer 18:1;O2/24:0[M[2]H7]
er 18:1;O2/26:1	676.6 -> 264.2	7.0	Cer 18:1;O2/24:0[M[2]H7]
Ser 18:1;O2/16:0[M[2]H7]	545.5 -> 271.3	4.7	internal standard
Ser 18:1;O2/18:0[M[2]H7]	573.5 -> 271.3	5.2	internal standard
er 18:1;O2/24:0[M[2]H7]	657.6 -> 271.3	7.0	internal standard
Ser 18:1;O2/24:1[M[2]H7]	655.5 -> 271.3	6.4	internal standard
er 18:2;O2/16:0	536.5 -> 262.2	4.2	Cer 18:1;O2/16:0[M[2]H7]
er 18:2;O2/18:0	564.5 -> 262.3	4.8	Cer 18:1;O2/18:0[M[2]H7]
er 18:2;O2/20:0	592.6 -> 262.3	5.3	Cer 18:1;O2/18:0[M[2]H7]
Ser 18:2;O2/22:0	620.6 -> 262.3	5.9	Cer 18:1;O2/24:1[M[2]H7]
Ser 18:2;O2/24:0	648.6 -> 262.3	6.5	Cer 18:1;O2/24:0[M[2]H7]
er 18:2;O2/24:1	646.6 -> 262.3	5.9	Cer 18:1;O2/24:1[M[2]H7]
er 18:0;O3/16:0	556.5 -> 282.3	4.4	Cer 18:1;O2/16:0[M[2]H7]
Ser 18:0;O3/18:0	584.6 -> 282.4	5.0	Cer 18:1;O2/18:0[M[2]H7]
er 18:0;O3/20:0	612.6 -> 282.4	5.6	Cer 18:1;O2/18:0[M[2]H7]
er 18:0;O3/22:0	640.6 -> 282.4	6.1	Cer 18:1;O2/24:1[M[2]H7]
er 18:0;O3/24:0	668.7 -> 282.4	6.7	Cer 18:1;O2/24:0[M[2]H7]
er 18:0;O3/24:1	666.6 -> 282.4	6.1	Cer 18:1;O2/24:1[M[2]H7]
G 15:0_18:1[M[2]H7]	605.6 -> 299.3	5.4	internal standard
IG 16:0_16:0	586.5 -> 313.3	5.7	
			DG 15:0_18:1[M[2]H7]
G 16:0_18:1	612.6 -> 313.3	5.7	DG 15:0_18:1[M[2]H7]
G 16:0_18:2	610.5 -> 313.3	5.3	DG 15:0_18:1[M[2]H7]
G 18:1_18:1	638.6 -> 339.3	5.8	DG 15:0_18:1[M[2]H7]
G 18:1_18:2	636.6 -> 339.3	5.3	DG 15:0_18:1[M[2]H7]
G 18:2_18:2	634.5 -> 337.3	4.8	DG 15:0_18:1[M[2]H7]
lexCer 18:0;O2/16:0	702.6 -> 284.3	4.3	HexCer 18:1;O2/17:0
lexCer 18:0;O2/18:0	730.6 -> 284.3	4.9	HexCer 18:1;O2/17:0
lexCer 18:0;O2/20:0	758.6 -> 284.3	5.5	HexCer 18:1;O2/17:0
lexCer 18:0;O2/22:0	786.7 -> 284.3	6.0	HexCer 18:1;O2/17:0
lexCer 18:0;O2/24:0	814.7 -> 284.3	6.7	HexCer 18:1;O2/17:0
exCer 18:0;O2/24:1	812.7 -> 284.3	6.0	HexCer 18:1;O2/17:0
lexCer 18:1;O2/16:0	700.6 -> 264.3	4.2	HexCer 18:1;O2/17:0
exCer 18:1;O2/17:0	714.6 -> 264.3	4.4	internal standard
exCer 18:1;O2/18:0	728.6 -> 264.2	4.7	HexCer 18:1;O2/17:0
exCer 18:1;O2/20:0	756.6 -> 264.2	5.3	HexCer 18:1;O2/17:0
exCer 18:1;O2/22:0	784.7 -> 264.2	5.8	HexCer 18:1;O2/17:0
exCer 18:1;O2/24:0	812.7 -> 264.2	6.4	HexCer 18:1;O2/17:0
exCer 18:1;O2/24:1	810.7 -> 264.2	5.8	HexCer 18:1;O2/17:0
C 15:0_18:1[M[2]H7]	753.6 -> 184.1	4.3	internal standard
C 34:1	760.6 -> 184.1	4.5	PC 15:0_18:1[M[2]H7]
C 34:2	758.6 -> 184.1	4.1	PC 15:0_18:1[M[2]H7]
C 36:0	790.6 -> 184.1	5.6	PC 15:0_18:1[M[2]H7]
C 36:1	788.6 -> 184.1	5.1	PC 15:0_18:1[M[2]H7]
			(Continued on next



Cell MetabolismArticle

Continued			
target	transition	RT (min)	Internal Standard
PC 36:2	786.6 -> 184.1	4.6	PC 15:0_18:1[M[2]H7]
PC 36:3	784.6 -> 184.1	4.3	PC 15:0_18:1[M[2]H7]
PC 36:4	782.6 -> 184.1	4.0	PC 15:0_18:1[M[2]H7]
SM 18:0;O2/16:0	705.6 -> 184.1	4.2	SM 18:1;O2/18:1[M[2]H9]
SM 18:0;O2/18:0	733.6 -> 184.1	4.7	SM 18:1;O2/20:1[M[2]H9]
SM 18:0;O2/20:0	761.6 -> 184.1	5.3	SM 18:1;O2/22:1[M[2]H9]
SM 18:0;O2/22:0	789.7 -> 184.1	5.8	SM 18:1;O2/24:1[M[2]H9]
SM 18:0;O2/24:0	817.7 -> 184.1	6.4	SM 18:1;O2/24:1[M[2]H9]
SM 18:0;O2/24:1	815.7 -> 184.1	5.8	SM 18:1;O2/24:1[M[2]H9]
SM 18:1;O2/14:0	675.5 -> 184.1	3.5	SM 18:1;O2/16:1[M[2]H9]
SM 18:1;O2/16:0	703.6 -> 184.1	4.0	SM 18:1;O2/18:1[M[2]H9]
M 18:1;O2/16:1[M[2]H9]	710.6 -> 193.1	3.6	internal standard
SM 18:1;O2/17:0	717.6 -> 184.1	4.2	SM 18:1;O2/18:1[M[2]H9]
SM 18:1;O2/18:0	731.6 -> 184.1	4.5	SM 18:1;O2/20:1[M[2]H9]
SM 18:1;O2/18:1[M[2]H9]	738.6 -> 193.1	4.0	internal standard
SM 18:1;O2/20:0	759.6 -> 184.1	5.1	SM 18:1;O2/22:1[M[2]H9]
SM 18:1;O2/20:1[M[2]H9]	766.7 -> 193.1	4.5	internal standard
SM 18:1;O2/22:0	787.7 -> 184.1	5.6	SM 18:1;O2/24:1[M[2]H9]
SM 18:1;O2/22:1[M[2]H9]	794.7 -> 193.1	5.1	internal standard
SM 18:1;O2/24:0	815.7 -> 184.1	6.2	SM 18:1;O2/24:1[M[2]H9]
M 18:1;O2/24:1	813.7 -> 184.1	5.6	SM 18:1;O2/24:1[M[2]H9]
M 18:1;O2/24:1[M[2]H9]	822.7 -> 193.1	5.6	internal standard
SPB 18:0;O2	302.3 -> 284.2	2.1	SPB 18:1;O2[M[2]H7]
SPB 18:1;O2	300.3 -> 282.3	2.0	SPB 18:1;O2[M[2]H7]
SPB 18:1;O2[M[2]H7]	307.3 -> 289.3	2.0	internal standard
G 15:0_15:0_18:1[M[2]H7]	829.8 -> 570.5	8.3	internal standard
G 48:0 [NL-16:0]	824.8 -> 551.5	8.4	TG 15:0_15:0_18:1[M[2]H7
G 48:1 [NL-18:1]	822.8 -> 523.5	8.3	TG 15:0_15:0_18:1[M[2]H7
G 48:2 [NL-14:1]	820.8 -> 577.6	8.3	TG 15:0_15:0_18:1[M[2]H7
G 48:2 [NL-16:0]	820.8 -> 547.5	8.2	TG 15:0_15:0_18:1[M[2]H7
G 48:2 [NL-16:1]	820.8 -> 549.5	8.2	TG 15:0_15:0_18:1[M[2]H7
G 48:2 [NL-18:1]	820.8 -> 521.5	8.2	TG 15:0_15:0_18:1[M[2]H7
G 48:3 [NL-16:1]	818.8 -> 547.5	8.1	
G 48:3 [NL-18:2]	818.8 -> 521.5		TG 15:0_15:0_18:1[M[2]H7 TG 15:0_15:0_18:1[M[2]H7
G 49:1 [NL-15:0]		8.1 8.4	
-	836.8 -> 577.5 836.8 -> 563.5	8.4	TG 15:0_15:0_18:1[M[2]H7
·G 49:1 [NL-16:0] ·G 49:1 [NL-18:1]			TG 15:0_15:0_18:1[M[2]H7
•	836.8 -> 537.5	8.4 8.5	TG 15:0_15:0_18:1[M[2]H7
G 50:0 [NL-18:0] G 50:1 [NL-14:0]	852.8 -> 551.5		TG 15:0_15:0_18:1[M[2]H7
• •	850.8 -> 605.6	8.4 8.4	TG 15:0_15:0_18:1[M[2]H7
G 50:1 [NL-18:1]	850.8 -> 551.5		TG 15:0_15:0_18:1[M[2]H7
G 50:2 [NL-18:0]	848.8 -> 547.5	8.4	TG 15:0_15:0_18:1[M[2]H7
G 50:2 [NL-18:1]	848.8 -> 549.5	8.3	TG 15:0_15:0_18:1[M[2]H7
G 50:2 [NL-18:2]	848.8 -> 551.5	8.4	TG 15:0_15:0_18:1[M[2]H7
G 50:3 [NL-14:1]	846.8 -> 603.6	8.3	TG 15:0_15:0_18:1[M[2]H7
G 50:3 [NL-16:1]	846.8 -> 575.6	8.3	TG 15:0_15:0_18:1[M[2]H7
G 50:3 [NL-18:1]	846.8 -> 547.5	8.3	TG 15:0_15:0_18:1[M[2]H7
G 50:4 [NL-14:0]	844.8 -> 599.5	8.2	TG 15:0_15:0_18:1[M[2]H7
G 51:0 [NL-16:0]	866.8 -> 593.6	8.5	TG 15:0_15:0_18:1[M[2]H7
ΓG 51:1 [NL-18:1]	864.8 -> 565.5	8.4	TG 15:0_15:0_18:1[M[2]H7

Article



Continued			
target	transition	RT (min)	Internal Standard
TG 51:2 [NL-15:0]	862.8 -> 603.6	8.4	TG 15:0_15:0_18:1[M[2]H7]
TG 51:2 [NL-16:0]	862.8 -> 589.6	8.4	TG 15:0_15:0_18:1[M[2]H7]
TG 51:2 [NL-18:1]	862.8 -> 563.5	8.4	TG 15:0_15:0_18:1[M[2]H7]
TG 52:1 [NL-18:0]	878.8 -> 577.5	8.5	TG 15:0_15:0_18:1[M[2]H7]
TG 52:2 [NL-16:0]	876.8 -> 603.6	8.4	TG 15:0_15:0_18:1[M[2]H7]
TG 52:3 [NL-16:1]	874.8 -> 603.6	8.3	TG 15:0_15:0_18:1[M[2]H7]
TG 52:3 [NL-18:2]	874.8 -> 577.6	8.3	TG 15:0_15:0_18:1[M[2]H7]
TG 52:4 [NL-16:0]	872.8 -> 599.6	8.3	TG 15:0_15:0_18:1[M[2]H7]
TG 52:4 [NL-18:1]	872.8 -> 573.6	8.3	TG 15:0_15:0_18:1[M[2]H7]
TG 53:2 [NL-17:0]	890.8 -> 603.6	8.5	TG 15:0_15:0_18:1[M[2]H7]
TG 54:0 [NL-18:0]	908.9 -> 607.6	8.6	TG 15:0_15:0_18:1[M[2]H7]
TG 54:1 [NL-18:1]	906.9 -> 607.6	8.6	TG 15:0_15:0_18:1[M[2]H7]
TG 54:2 [NL-18:0]	904.9 -> 603.6	8.5	TG 15:0_15:0_18:1[M[2]H7]
TG 54:3 [NL-18:1]	902.9 -> 603.6	8.4	TG 15:0_15:0_18:1[M[2]H7]
TG 54:4 [NL-18:0]	900.8 -> 599.5	8.4	TG 15:0_15:0_18:1[M[2]H7]
TG 54:4 [NL-18:2]	900.9 -> 603.9	8.3	TG 15:0_15:0_18:1[M[2]H7]
TG 54:5 [NL-18:1]	898.9 -> 599.6	8.3	TG 15:0_15:0_18:1[M[2]H7]
TG 54:6 [NL-18:2]	896.9 -> 599.6	8.2	TG 15:0_15:0_18:1[M[2]H7]
TG 56:6 [NL-20:4]	924.9 -> 603.6	8.3	TG 15:0_15:0_18:1[M[2]H7]
TG 56:8 [NL-20:4]	920.9 -> 599.6	8.2	TG 15:0_15:0_18:1[M[2]H7]
TG 58:8 [NL-22:6]	948.9 -> 603.7	8.3	TG 15:0_15:0_18:1[M[2]H7]

Laser Capture Microdissection and RNA Seq

Laser capture microdissection was performed as previously described. ⁸⁹ Briefly, the duodenum of the small intestines from male B6 mice with different microbiotas (GF, SPF on autoclave diet, SF) were dissected out, cleaned, and flushed with OCT and placed in cryo mold, and embed in OCT (Fisher 23-730.571). Frozen sections 9 um thick were cut from the blocks and mounted on PEN slides. Working one slide at a time, slides were taken out of the freezer, fixed with 70% EtOH, stained with Methyl Green and Eosin Y, dehydrated in xylene. Laser capture microdissection of IECs was performed using an ZEISS PALM MicroBeam Platform. 5000-10000 cells were obtained from each section in one hour. After tissue was collected 350μL of Qiagen buffer RLT+ beta mercaptone ethanol was added and incubated at room temperature for 30 min for lysis before being stored in the -80 °C. RNA was extracted with the RNeasy micro kit (Qiagen 74004) with on column DNase I digest and eluted in 14μL RNAse free H2O. Samples have been stored at -80 °C. Table S6 for RNA seq QC and full QC details available under BioProject PRJNA1122642 and GEO GSE269607.

Host RNA seq analysis with GSEA

Raw counts from DESeq2 processed data was uploaded to GSEA software, a joint project of UC San Diego and Broad Institute. ^{90,91} Wiki pathway analysis of gene sets for sphingolipid metabolism overview and sphingolipid metabolism integrated pathways.

RNA seq and analysis of Turicibacter culture

Total RNA extracted from *Turicibacter* KKT8 samples grown in Schaedler's media alone or with 12.5 μM PA were hybridized with NEBNext rRNA Depletion Solution (bacteria) (E7850L) to substantially diminish rRNA from the samples. Stranded RNA-seq libraries were prepared using the NEBNext Ultra II RNA Library Prep Kit for Illumina (E7770L). Purified libraries were qualified on an Agilent Technologies 2200 TapeStation using a D1000 ScreenTape assay (cat# 5067-5582 and 5067-5583). The molarity of adapter-modified molecules was defined by quantitative PCR using the Kapa Biosystems Kapa Library Quant Kit (cat#KK4824). Individual barcoded libraries were normalized to 10 nM and equal volumes were pooled in preparation for Illumina sequencing.

Raw reads were first quality and adapter trimmed with fastp, then aligned with HiSat2 (v2.1.0) to the *Turicibacter* KK003 genome (GCF_037014675.1) with the "-no-spliced-alignment" and "-no-discordant" flags.^{92,93} Alignments were then sorted and indexed with samtools⁹⁴ Counts of all CDS features were generated from alignments using FADU to more accurately model counts of pro-karyotic alignments.⁹⁵ Feature counts were then imported into R with tximport function in the tximeta package and a DESeq dataset object created before differential abundance testing with DESeq2 and log2 fold change shrinkage with ashr.^{81,96,97} Prior to differential abundance testing, features not detected in at least 2 samples with more than 10 counts were removed resulting in 2001 features ultimately tested. FACoP.v2 from the FUNAGE-Pro software was used to add annotations to the reference genome including operon predictions.⁸² The ComplexHeatmap package was used for plotting the heatmap of top differentially abundant genes.⁹⁸





Turicibacter Genome Analysis for SPT, CerS and Fatty Acid Biosynthesis Pathway

A hidden Markov model (HMM) was constructed for bacterial serine palmitoyltransferase (SPT) proteins. Briefly, SPT proteins previously described ⁹⁹ were combined with a collection of bacterial SPT proteins downloaded from UniProt (February 19, 2024). Duplicate sequences were removed and sequences were aligned using the E-INS-I method in MAFFT v. 7.511. ¹⁰⁰ Sequences shorter than 250 amino acids were removed, and the remainder were realigned and then passed through MaxAlign. This resulted in a multiple sequence alignment of 272 sequences with 373 gap-free sites. 204 of these sequences (75%) were randomly selected and used to build the HMM model using the hmmbuild program in HMMER (v. 3.3.2; http://hmmer.org), validated using the remaining 25% of sequences. The Panther model for bacterial ceramide synthase (CerS), PTHR41368.orig.30.pir, was downloaded and used to search for proteins with CerS homology. The hmmsearch program in HMMER (v. 3.3.2) was used to search both models against proteins annotated in the *Turicibacter* KKT8 genome.

To assess the presence of genes in the KKT8 genome known to be in the fatty acid biosynthesis pathway, all protein sequences were analyzed with GhostKOALA to add KEGG ontology annotation and paint the genes present onto the KEGG fatty acid biosynthesis pathway (ko00061).¹⁰¹ Additionally, to visualize genes involved in Fatty acid biosynthesis IMG/M KEGG mapping analysis of *Turicibater* KK03 was used.

Metagenomic sequencing and analysis of SF community

Spore former communities were analyzed by shotgun metagenomic sequencing of DNA isolated from 4 samples from the same isolator. 2 fecal samples and 2 small intestinal contents samples were collected and processed with 2 different DNA extraction methods (Qiagen PowerFecal pro- cat# 51804 and Zymoresearch HostZERO microbial DNA kit; cat #D4310) to maximize bacterial reads from small intestinal contents. Illumina Libraries were constructed at the Huntsman Cancer Institute High-thoughput genomics facility using the Nextera DNA Flex Library Prep kit (cat#20025520) with an average insert size of 450 bp. PCR-amplified libraries were qualified on an Agilent Technologies 2200 TapeStation using a D1000 ScreenTape assay (cat# 5067-5582 and 5067-5583) and the molarity of adapter-modified molecules was defined by quantitative PCR using the Kapa Biosystems Kapa Library Quant Kit (cat#KK4824) and then sequenced on a NovaSeq with paired-end 150 cycle sequencing.

Reads were adapter and quality trimmed, host read filtered (GRCm39 *Mus musculus* assembly) and then taxonomically assigned with Kraken2 and the "plusPF" RefSeq Index (version 6/5/2024) within the taxprofiler nextflow-core pipeline. Sankey plots were created with the pavian metagenomics explorer, excluding any remaining host reads. Sankey plots were created with the pavian metagenomics explorer, excluding any remaining host reads.

QUANTIFICATION AND STATISTICAL ANALYSIS

Before quantification individual data points were anonymized. A power of 80%, a significance level of 0.05, and variance and effect was estimated from preliminary experiments and used to estimate the sample size for all experiments. Mouse experiments contained approximately 3-10 for biological replicates or individual treatment groups. Smaller groups were limited by material. *In vivo* and experiments were repeated 3 times, where appropriate datasets of biological and technical replicates were pooled. Our data in the paper in the figures are represented as bar graphs showing the individual data points and SD. The only case in which outliers were removed were in the human gut microbiota metagenomic showing *Turicibacter* abundance. In this case outliers were removed according to the ROUT method for robust regression and outlier removal developed in GraphPad PRISM using a Q score of 1%. GraphPad Prism 8 was also used to calculate Student's unpaired t-test with equal variance assumptions when comparing two groups. A 1-way or 2-way ANOVA was used to compare multiple groups. A p-value of 0.05 was required to reject the null hypothesis that no difference existed between groups.